Nonlinear radiative MHD Williamson nanofluid flow over a stretching cylinder in a Darcy- Forchheimer porous medium

Thesis Submitted By

Muhammad Usman Khan
(01-248182-008)

Supervised By

Prof. Dr. M. Ramzan

A dissertation submitted to the Department of Computer Science, Bahria University, Islamabad as a partial fulfillment of the requirements for the award of the degree of MS(Mathematics)

Session (2018 - 2020)

Bahria University
Discovering Knowledge

MS-13

Thesis Completion Certificate

Student's Name: Muhammad Usman Khan Registration No. 59379
Program of Study: MS(Mathematics)
Thesis Title: "Nonlinear radiative MHD Williamson nanofluid flow over a stretching cylinder in a Darcy-Forchheimer porous medium"

It is to certify that the above student's thesis has been completed to my satisfaction and, to my belief, its standard is appropriate for submission for Evaluation. I have also conducted plagiarism test of this thesis using HEC prescribed software and found similarity index at 16% that is within the permissible limit set by the HEC for the MS/MPhil degree thesis. I have also found the thesis in a format recognized by the BU for the MS/MPhil thesis.

Principal Supervisor's Signature ____________________

Date: 30-09-2020 Name: Prof. Dr. M. Ramzan

Dedicated to

My beloved parents and respected supervisor

Acknowledgments

Words are bound and knowledge is limited to praise **ALLAH** the beneficent, the merciful who universe and bestowed mankind with the knowledge and ability to think into his secrets. Then the trembling lips and wet eyes praise the greatest man of universe, the last messenger of **ALLAH, HAZRAT MUHAMMAD (PBUH)**, whom **ALLAH** has sent as mercy for worlds, the illuminating torch, the blessing for the literate, illiterate, rich, poor, powerful, weaker, and able and disable.

My acknowledgment is to my kind, diligent and highly zealous supervisor, Prof. Dr. M. Ramzan, who supported me with his cherished opinions and inspirational discussions. His valuable expertise, comments, suggestions and instructions are most welcome that greatly improved the clarity of this document.

My gratitude is to my honorable professors who took me to the apex of my academia with their guidance. In particular, Dr. Rizwan-ul-haq and Dr. Jafar Hasnain who have always been supportive in all of my course work and kept encouraging me throughout the session in Bahria University, Islamabad Campus. They are the true teachers who have made Mathematics Department of BUIC, a real place of learning.

My intense recognition is to my father, mother, brothers and sister, who are always real pillars for my encouragement and showered their everlasting love, care and support throughout my life. I am very grateful to Ma’am Hina Gul and Ma’am Saima who support and guided me at every stage, my seniors Sania Naseer and Nazia Shahmir, and my friend Hafeez Akhter were specially remained enormously helpful throughout the period of my MS studies.

Muhammad Usman Khan
Bahria University Islamabad, Pakistan
September 2020

Bahria University
Discovering Knowledge

MS-14A

Author's Declaration

I, **Muhammad Usman Khan** hereby state that my MS thesis titled **"Nonlinear radiative MHD Williamson nanofluid flow over a stretching cylinder in a Darcy-Forchheimer porous medium"** is my own work and has not been submitted previously by me for taking any degree from this university **Bahria University Islamabad** or anywhere else in the country/world.

At any time if my statement is found to be incorrect even after my Graduate the university has the right to withdraw/cancel my MS degree.

Name of scholar: **Muhammad Usman Khan**

Date: **30/09/2020**

Bahria University
Discovering Knowledge

MS-14B

Plagiarism Undertaking

I solemnly declare that research work presented in the thesis titled "**Nonlinear radiative MHD Williamson nanofluid flow over a stretching cylinder in a Darcy-Forchheimer porous medium**" is solely my research work with no significant contribution from any other person. Small contribution / help wherever taken has been duly acknowledged and that complete thesis has been written by me.

I understand the zero tolerance policy of the HEC and Bahria University towards plagiarism. Therefore I as an Author of the above titled thesis declare that no portion of my thesis has been plagiarized and any material used as reference is properly referred / cited.

I undertake that if I am found guilty of any formal plagiarism in the above titled thesis even after award of MS degree, the university reserves the right to withdraw / revoke my MS degree and that HEC and the University has the right to publish my name on the HEC / University website on which names of students are placed who submitted plagiarized thesis.

Student / Author's Sign: ____________________

Name of the Student: **Muhammad Usman Khan**

Abstract

This mathematical analysis refined, a non-linear radiative magnetohydrodynamic (MHD) Williamson nanofluid flow via a stretching cylinder. Effects of Darcy-Forchheimer porous media is also discussed. Flow analysis is performed in the presence of partial slip boundary condition. The requisite boundary layer equations are converted into the non-linear ODEs using suitable transformations. The resulting system of linear equations is addressed by bvp4c built-in function of MATLAB scheme. The outcomes of the prominent parameters versus involved profiles are portrayed and conversed in light of their physical significance. The results obtained in the analysis are substantiated by erecting a comparative table with an established result in the literature. An outstanding matching is achieved in this regard.

List of Tables

List of Figures

Symbols

x, r	Coordinate axis
u, v	Velocity components
μ	Absolute viscosity
τ_{yx}	Shear force
ρ	Density
α	Thermal diffusivity
k	Thermal conductivity
ν	Kinematic viscosity
c_p	Specific heat capacity
q	Heat transfer rate
η	Similarity variable
A	Area
ΔT	Temperature difference
$\frac{du}{dy}$	Velocity gradient
η_1	Apparent viscosity
s	Index of consistency
n	Reaction order
m	Mass of substance
V	Volume

P	Pressure
F_1	Force
$\frac{dT}{dx}$	Temperature gradient
e	Emissivity of the system
h	Coefficient of heat transfer
T_s	System temperature
T_∞	Ambient fluid temperature
T_w	Wall’s temperature
T	Fluid temperature
υ_f	Forchheimer velocity
k_1	Inertial permeability
k^*	Mean absorption coefficient
$\Pr$	Prandtl number
Rd	Radiation parameter
u_w	Stretching velocity
u_0	Reference velocity
l	Characteristic length
Cf_x	Skin friction
Nu_x	Local Nusselt number
Nn_x	Density number of motile microorganism
Sh_x	Local Sherwood number
q_w	Wall heat

J_w	Mass flux
Nt	Thermophoresis parameter
D_T	Thermophoretic diffusion coefficient
τ	Stress tensor
N_b	Brownian motion parameter
D_B	Brownian diffusion coefficient
D_m	Coefficient of mass diffusion
C	Fluid concentration
C_w	Wall's concentration
C_∞	Ambient fluid concentration
Sc	Schmidt number
Fr	Forchheimer number
c_b	Drag coefficient
γ	Chemical reaction parameter
λ_1	Reaction rate
Pe	Peclet number
λ	Porosity parameter
w_c	Constant maximum cell swimming speed
D_n	Diffusivity of the microorganism
b	Body forces
We	Local Weissenberg number
q_n	Surface motile microorganism

k_2	Permeability of porous medium
ρ_f	Base liquid density
τ^*	Stress tensor
$\frac{D}{Dt}$	Material time derivative
L^*	Strain tensor
ρ_p	Density of nanoparticles
B_0	Magnetic field intensity
q_r	Radiative heat flux
ψ	Axisymmetric stream function
M	Curvature parameter
K	Magnetic interaction parameter
B_1	Wall roughness parameter
B_2	Wall thermal parameter
B_3	Concentration slip parameter
B_4	Motile slip parameter
θ_w	Temperature ratio parameter
Γ	Williamson parameter
F	Non-uniform inertial coefficient
Lb	Bioconvection Lewis number
σ_1	Electrical conductivity
σ^*	Stefan-Boltzmann constant
σ	Bioconvection parameter

L_1 Velocity slip coefficient

L_2 Thermal slip coefficient

L_3 Concentration slip coefficient

L_4 Motile slip coefficient

Contents

Chapter 1

Introduction and Literature review

1.1 Introduction

Nanofluid, an emerging field of engineering has caught the eye of numerous researchers who were looking at the ways to improve the efficiency of cooling processes in industries, Nanofluid is different from the other ordinary base fluids because nanoliquids are manufactured by inserting nanoparticles into the base liquid. The nanoliquid is a liquid that carries nanometer size (100nm) of particles, known as nanoparticles. The particles used in nanoliquids are commonly made up of metals, oxides, or carbon nanotubes. Generally, the common base liquids include water, ethylene glycol and oil. This fluid is different from other ordinary base fluids because it is prepared by dispersing nanoparticles into the base fluid. These nano sized particles are inserted into base fluids to improve the thermal performance and heat transfer efficiency of the flow. Nanoliquid is the ideal applicant to get position of working fluid. The increasing thermal performance that occurs by exceeding the base fluid and a size of $1-100$ nm nanoparticles, these two substances are employed to get greatest improvement into the thermal features under lower concentrations. Nanoliquids have potential to significantly enhance heat transfer rates in a variety of areas such as nuclear reactors, industrial cooling applications, transportation industry, heat exchangers, micro-electromechanical systems, fiber and granular insulation, chemical catalytic reactors, packed blood flow in the cardiovascular system engaging the Navier–Stokes equation. Advanced thermal features of the naofluid are imperative in many fields like pharmaceutical, transportation, microelectronics, micromanufacturing, power generation, thermal therapy for cancer surgery, air-conditioning, metallurgical and chemical engineering fields etc. In vehicles, the demand for nanofluids as coolants looks good in size and as a result this consumes less energy to control road resistance. Due to the significant advancement in automotive aerodynamics, there is great interest in breaking down systems by direct heat dissipation. Many investigators have recently added some work to promote solar collectors with highly absorpation of solar radiation.

Recent developments in industrial applications have introduced a broad variety of non-Newtonian liquids that are different by various prespectives from other viscous liquids. All those liquids in which the rate of shear is changed and the pressure of shear does not changed is considered to be non-Newtonian. Thus, this difference in shear strength results to alter the viscosity of these liquids, also known as the "apparent viscosity" of the liquid. Richardson and Chhabra in 2018 described a non-Newtonian liquid, whose flow path (shear stress vs. shear rate) is either nonlinear or that don't pass through the origin, which means that the apparent viscosity is not remain same at a given pressure and temperature. These liquids are generally divided into three categories as time dependent, viscoelastic and time independent liquids. Numerous things we use in our everyday life happen due to these kinds of liquids, Such that shampoo, toothpaste, sillyputty and whiped cream etc. It is renowned that mechanics of non-Newtonian liquids offer a certian challenge to mathematiciains and technologists. The nonlinearity may appear itself in numerous aspects in different fields such as biological-engineering and drilling operations. The Navier-Stokes approach is insufficient for such liquids and no single fundamental equation is provided in the literature which demonstrates the characteristics of all fluids. Thus, several non-Newtonian fluid models have been introduced. Rheological characteristics of non-Newtonian liquids differ a lot than the Newtonian liquids. No doubt, the rheological properties of all the non-Newtonian liquids can not be predicted by one constitutive equation joining rate of shear and rate of strain. As for non-Newtonian liquids, there always a nonlinear relationship between the shear rate and strain rate. The constitutive equations in non-Newtonian liquids are much complex, nonlinear and of higher order as compared to Newtonian liquids. These liquids can be divided by three main categories:

- Liquids that shows the rate of shear at any point is determined solely by the amount of shear stress at that time; those liquids are variously called "time independent", "inelastic", "purely viscous" or "generlized Newtonian liquids".

- Complex liquids are related to the shear stress and rate of shear depends, more to the time period of shearing and their kinematic history; are known as "time dependent liquids".
- Materials exhibiting the properties of both ideal liquids and elastic solids and showed partial elastic recovery and after the deformation this is classified as "visco-elastic liquids".

This division procedure is compulsory most of the real substances tend to show the combination of two or three kinds of non-Newtonian properties. These properties are too broader to be tackled in the early stages of constructing the model. Therefore, a specific rheological model will be choosen for initial use of development to deviating from the assumed model. Several approximate and self-consistent non-Newtonian rheological models have been performed over the past decades as no one can incorporate the specific features of every fluid. These models are classified into different models such that rate type and integral type models. In particular, different types of fluid models have been introduced in recent era such as Williamson liquid model, Carreau liquid model or Burgers liquid model etc. The Williamson fluid is characteristic of a non-Newtonian liquid model with shear thinning characteristics.

The term Darcy-Forchheimer comes from the law of Darcy which interprets the liquid flow along a spongy channel. This law was originated and dependent upon the consequences of analysis on the water flow across the beds of sand. Movements in spongy medium in which inertial effects are prominent comes with the variations of Reynolds numbers. Therefore, this introductary term is added to Darcy equation and is referred to as Darcy-Forchheimer term. This term represents the non-linear behavior of the flow data versus pressure difference. With wide utilization of grain stockpiling, petroleum technology, frameworks of ground water and oil assests, this Darcy law is of immense importance in the field of Fluid Mechanics. Places where the porous medium has larger flow rates due to non-uniformity, such as near the wall, Darcy law is not applicable.

1.2 Literature review

Nanoliquid has been explored and discussed by many investigators because of its distinctive properties and is known as the suspended colloidal liquid with nano-size metallic or non-metallic particles. As Choi et al. [1] found that the incorporation of nanoparticles to the base fluids significantly enhance their thermal efficiency. The rising demand for highly efficient cooling devices encourage Koo and Kleinstreuer [2] to study the steady laminar nanofluid flow in micro heat sinks. It is noticed that very low nanoparticle concentration in nanofluids, it results in a higher thermal conductivities that exhibits a remarkable state of nanofluids [3-4]. Ramzan et. al [5] explored the numerical study of radiative Williamson nanoliquid flow via a convectively heated Rigid plate with chemical reaction. Hayat et. al [6] investigated Darcy–Forchheimer flow of three-dimensional Williamson nanoliquid over an extended heated nonlinear stretched surface. Various researchers revealed the numerous aspects of the Williamson nanoliquid [7-15].

The material with stomata is termed as porous medium. It includes a large number of applications such that oil production, water flow in reservoirs and catalytic vessels etc. The idea of the flow of a liquid past a permeable media was first given by a French, Darcy [16] in 1856. But this notion couldn't be so popular owing to its limitations of smaller porosity and low velocity. Subsequently, Forchheimer [17] modify the momentum equation with the addition of the square velocity condition into the Darcian velocity to address the obvious deficiency. This was later named by Muskat [18] as "Forchheimer term" which is true of the high Reynolds number. Mondal and Pal [19] deliberated the Darcy-Forchheimer model over porous media past the linearly extended surface and concluded that concentration distribution is diminishing function of the electric field parameter. The flow of the hydromagnetic nanofluid past the Darcy-Forchheimer media forum on the impact of second order boundary condition is numerically evaluated by Ganesh et al. [20]. Alshomrani et al.[21] discussed the 3D Darcy-Forchheimer model with carbon nanotubes and the homogeneous heterogeneous reactions. The viscous nanofluid with Darcy-Forchheimer effect past curved surface is analyzed by Saif et al. [22]. Seth et al. [23] scrutinized numerically the flow of carbon nanotubes over a permeable Darcy-Forchheimer media in a rotating frame and many therein [24-28].

Chemical reaction can be explained as an interaction joining two or more chemicals that produces one or more newly chemical compounds. Many chemical reactions requires accelerator and heat (*i.e.* catalyst). A chemical reaction in that catalyst is in the same phase (*i.e.* in the same state of matter) as the reactant(s) are called homogeneous catalytic reaction. Reactions joining with two gases, and two liquids which makes the mixture of household cooking gas with oxygen gas leading to flame are typical examples of homogeneous catalytic reactions. In heterogeneous catalytic reaction, catalyst and reactants are in different phases (*i.e.* different states of matter). Examples of heterogeneous catalytic reactions are chemical reactions between a gas and a liquid, a gas and a solid, and liquid and a solid. Investigation of activation energy in Couette-Poiseuille flow of nanoliquid in the existence of chemical reaction and convective boundary conditions is discussed by Zeeshan et al. [29]. Animasaun [30-32] explored flow of chemically reacting liquid via binary mixture in flow of micropolar liquid, nth order of chemical reaction in Casson liquid flow and quartic autocatalytic chemical reaction in 47 nm alumina-water nanoliquid within boundary layer. In prespective of its clarity, the remarkable work of current researchers, see few studies [33-42].

Chapter 2

Basic preliminaries and laws

This chapter includes some standard definition basic concepts and fundamental equations.

2.1 Fluid

A material consist of a particles those deforms continuously under the influence of shear stress is known as fluid. Paints, water, cooking oil, blood and shampoos are examples of fluids.

2.2 Fluid mechanics

The main class of mecahnics which study the effects of fluid. It can be classified into two subclasses.

2.2.1 Fluid statics

A subclass of fluid mechanics related to examine the conditions under which fluid is at rest is known as fluid statics.

2.2.2 Fluid dynamics

A subclass of fluid mechanics that is related to examine the conditions when fuid is in motion called fluid dynamics.

2.3 Flow

Flow is defined as a material that deforms smoothly and fluently under the effect of different kinds of forces. Flow is further divided into two major subclasses.

2.3.1 The Laminar flow

When fluid flows in the way that different layers of fluid never cross each other and have constant velocity at every point in the flow field.

2.3.2 The Turbulent flow

When fluid flow in the way that different layers of fluid cross each other and have irregular velocities in the flow field.

2.4 Viscosity

It is the primary characteristic of fluid that describe the behavior and motion of the fluid nearby the boundary. When fluid is deforms by shear stress then an internal quantity generate that measures the fluid flow resistance. Mathematically, can be represented as follows:

$$\text{viscosity } (\mu) = \frac{\text{shearstress}}{\text{gradient of velocity}}. \tag{2.1}$$

2.4.1 Dynamic viscosity

It is defined as the measure of the fluid inner flow resistance. Its SI unit is kg/ms.

2.4.2 Kinematic viscosity

The ratio of the absolute viscosity (μ) and the liquid mass density (ρ) is defined as kinematic viscosity. Mathematically,

$$\upsilon = \frac{\mu}{\rho}. \tag{2.2}$$

2.5 Thermal diffusivity

The thermal diffusivity is a material specific property for describing the heat conduction. This value express how speedily a material reply to change in temperature. It is the proportion of thermal conductivity to a certain amount of heat capacity and density. Mathematically,

$$\alpha = \frac{k}{\rho c_p}, \tag{2.3}$$

where c_p the certain amount of heat capacity, ρ is density whereas k is the thermal conductivity.

2.6 Thermal conductivity

It is a measurement of the capacity of a specific substance to conduct heat. To the Fourier law of heat conduction " The ratio of heat transfer rate (q) through a material of unit thickness (d) times unit cross section area (A) and unit temperature difference (ΔT)". Mathematically, written as:

$$k = \frac{qd}{A(\Delta T)}. \tag{2.4}$$

In SI system thermal conductivity has unit $\frac{W}{m.K}$.

2.7 Density

It is expressed as the mass of a material per unit volume. This quantity used to calculate that how much stuff of a material present in a unit volume.

Mathematically,

$$\rho = \frac{m}{V}, \tag{2.5}$$

where m is the mass of the substance and V is the volume. In SI system units it is calculated as kg/m^3.

2.8 Pressure

A force applied perpendicular to the surface per unit area.

Mathematically pressure is given by:

$$P = \frac{F_1}{A}. \tag{2.6}$$

The SI unit of pressure is Nm^{-2}.

2.9 Newton law of viscosity

Those fluid which show the direct and linear corrspondence between gradient of velocity and shear stress. Mathematically, it can be represented as follows:

$$\tau_{yx} \propto \frac{du}{dy}, \tag{2.7}$$

or

$$\tau_{yx} = \mu \left(\frac{du}{dy} \right), \tag{2.8}$$

in which τ_{yx} denotes the force of shear applied on the fluid's element and μ the absolute viscosity.

2.10 Newtonian fluids

The liquids which follow the expression for Newton viscosity law. Here, direct and linear relationship exists between velocity gradient and shear stress. Sugar solutions, water, glycerine and silicone oils are common examples of this liquids.

2.11 non-Newtonian fluids

The liquids that do not follow the expression for Newton viscosity law. Here, a nonlinear relationship exists between velocity gradient and shear stress. Mathematically

$$\boldsymbol{\tau}_{yx} \propto \left(\frac{du}{dy}\right)^{n}, \; n \neq 1, \tag{2.9}$$

or

$$\boldsymbol{\tau}_{yx} = \eta_1 \frac{du}{dy}, \; \eta = s\left(\frac{du}{dy}\right)^{n-1}, \tag{2.10}$$

where η_1 is termed as apparent viscosity, $\boldsymbol{\tau}_{yx}$ the shear stress, s denotes the index of consistency, and n is the index of flow behaviour. For $n = 1$, Eq. (2.10) shows the Newton law of viscosity. Honey, tooth paste and mayonnaise are common examples of this fluid.

2.12 Porous surface

It is a material which made out of pores, over which fluid or gas can travel through. Few examples are biological tissues, cork and rocks. Sponges, fabrics, ceramics and foams are also gathered for the purpose of porous media.

2.13 Porosity

The measure of spongy space in a porous substance is known as porosity.

2.14 Permeability

It is the strength of a porous substance to allow fluid to travel through it. Those materials which have low porosity are minor permeable while materials having large pores are easily permeated have high porosity.

2.15 Mechanism of heat flow

A form of energy that moves from warmer to colder system. Flow of heat takes place between two objects when they are at different temperatures.The dispersion of heat takes place in any one of the following three ways:

2.15.1 Conduction

A procedure in which heat flows from the hot area to the cool area of a liquids and solids because of the collisions of free electrons and molecules is called conduction. Mathematically

$$\frac{\boldsymbol{q}}{A} = k\left(\frac{T_1 - T_2}{X_1 - X_2}\right) = k\frac{\Delta T}{\Delta X}, \tag{2.11}$$

where

$$\boldsymbol{q} = -kA\frac{dT}{dx}, \tag{2.12}$$

in which $\boldsymbol{q}$ represents the heat flow, A the area of the surface, k the thermal conductivity, T_1 temperature is greater than T_2, $\frac{dT}{dx}$ denotes the temperature gradient and negative sign shows that heat is conducted from greater to low temperature.

2.15.2 Radiation

It is a process where heat is supplied by means of electromagnetic waves. This phenomenon plays vital role in heat transfer in vaccum.Mathematically

$$q = e\sigma^* A \left(\Delta T\right)^4,$$

where q denotes the heat transfer, e for emissivity of the system, σ^* for Stefen-Boltzmann's constant, A for area and $(\Delta T)^4$ for the temperature difference between two systems of fourth power.

2.15.3 Convection

A phenomenon in which heat flows from the hot area to the cool area of liquids and gases due to the motion of molecules is said to be convection. Mathematically,

$$q = hA\left(T_s - T_\infty\right), \tag{2.13}$$

where h is coefficient heat transfer (convective), T_s for system temperature, A for area and T_∞ for the ambient temperature.

2.16 Nanofluid

A liquid that has very small metallic particles in it (called nanometer particles) is said to be Nanofluid. These liquids are formed by the colloidal suspensions of nanoparticles in the conventional liquid. The nanoparticles employed in nanoliquids typically are nanotubes, oxides and metals. Most ordinary base fluids are oil and water.

2.17 Darcy law

It interprets the flow of a liquid through a spongy medium. This law is originated and dependent on the consequences of analysis into the water flow across the beds of sand. It additionally models the scientific basis of fluid permeability needed in the Geo sciences.

2.18 Darcy-Forchheimer Law

Movements in spongy medium with Reynolds numbers greater than 10, and in which inertial effects are prominant. So, this inertial term is add on the Darcy's eq. and is called as Forchheimer term. This term represents the non linear change of the pressure difference and flow of data.

$$\frac{\partial p}{\partial x} = \frac{\mu}{k^*}\upsilon_f - \frac{\rho}{k_1}\upsilon_f^2, \tag{2.14}$$

where k_1 represents inertial permeability and υ_f represents forchheimer velocity.

2.19 Non-dimensional parameters

2.19.1 Reynolds number

The significant non dimensionl number that is used to recognize that either the flow is laminar or is turbulent. It describes viscous and inertial forces ratio. Mathematically, this number is expressed as:

$$\begin{aligned} \mathrm{Re} &= \frac{\text{inertial forces}}{\text{viscous forces}}, \\ &= \frac{v \times l}{\upsilon}. \end{aligned} \tag{2.15}$$

Here, v depicts the velocity of fluid, l describe the characteristic length and υ represent kinematic viscosity. Reynolds number are utilized to describe distinct flow behaviours (laminar or turbulent flow) within a similar fluid. Laminar flow arises at small Reynolds number, in which we can note that viscous effects are eminent. Turbulent flow arises at high Reynolds number, where inertial effects are eminent.

2.19.2 Prandtl number

It expresses the ratio joining momentum diffusivity to the thermal diffusivity is called Prandtl number. Mathematically,

$$\begin{aligned} \mathrm{Pr} &= \frac{\upsilon}{\alpha}, \\ &= \frac{\mu c_p}{k}. \end{aligned} \tag{2.16}$$

in which μ denotes the dynamic viscosity, c_p represent the specific heat and k stands for thermal conductivity.

2.19.3 Radiation parameter

The combined contribution of conduction to the thermal radiation flow, which can be expressed as follows:

$$Rd = \frac{4\sigma^* T_\infty^3}{kk^*}, \tag{2.17}$$

where k^*denoes the mean absorption coefficient, k stands for temperature dependent thermal conductivity, T_∞ for ambient temperature and σ^*represent the Stefan-Boltzmann constant.

2.19.4 Skin friction coefficient

Liquid passing over a surface experiences certain amount of drag that is known as Skin friction. It takes place between the flowing liquid and the solid surface that causes decrement in the rate of flow of fluid. Mathematical expression for Skin friction is given as follows:

$$C_{f_x} = \frac{\mu \left(u_r + v_x\right)_{r=R}}{\rho u_w^2}, \tag{2.18}$$

in which ρ represents the density and u_w denotes the velocity at the wall.

2.19.5 Nusselt number

It expresses the proportion of convective to conductive heat transfers joining solid boundary and moving liquid is known as Nusselt number. Mathematically

$$Nu_x = \frac{xq_w}{k\left(T_w - T_\infty\right)}\ , \tag{2.19}$$

in which q_w represent the wall heat and k the thermal conductivity respectively.

2.19.6 Sherwood number

Sherwood number is a number which is mass trasfer at the wall.

$$Sh_x = \frac{xj_w}{D_m\left(C_w - C_\infty\right)} \tag{2.20}$$

in which j_w represent the mass flux and D_m the cofficient of mass diffusion respectively.

2.19.7 Thermophoresis parameter

Thermo diffusion is utilized to prevent the mixing of different mobile particles of liquid due to a pressure gradient or separate the mixture of particles after mixing up due to the presence of thermal gradients. Thermophoresis is positive for cold surface and it is negative for a hot surface.

Mathematically

$$Nt = \frac{\tau D_T (T_w - T_\infty)}{\upsilon T_\infty}, \tag{2.21}$$

where T_w and T_∞ denotes the wall's temperature and ambient temperature, D_T stand for thermophoretic coefficient and υ represents the kinematic viscosity.

2.19.8 Brownian motion parameter

Brownian motion appear due to size of the nanoparticles in a nanofluid. It is a nanoscale phenomenon that exhibits the thermal influences of nanofluid.

Mathematically,

$$Nb = \frac{\tau D_B (C_w - C_\infty)}{\upsilon}, \tag{2.22}$$

in the above equation τ is the proportion of effective heat and heat capacity of the nanoparticles and fluid respectively, υ denotes the kinematic viscosity. C_w stands for wall's concentration, C_∞ stands for ambient concentration and D_B represents Brownian diffusion coefficient.

2.19.9 Schmidt number

This dimensionless quantity can be defined as the proportion of non-Newtonian viscosity (kinematic) to mass diffusivity.

Mathematically

$$Sc = \frac{\upsilon}{D_B}, \tag{2.23}$$

where υ represents the kinematic viscosity and D_B stand for mass diffusivity.

2.19.10 Forchheimer number

The Farchheimer number is proposed to identify different flow patterns. This number is determined with the ratio of pressure gradient to the viscous resistance.

Mathematically,

$$Fr = \frac{c_b}{\sqrt{k_2}}, \tag{2.24}$$

with c_b represent Drag coefficient and k_2 the permeability of porous medium.

2.19.11 Chemical reaction parameter

The non-dimensional parameter used to measure the strenght of chemical reaction rate is called chemical reaction parameter and can be written as:

$$\gamma = \frac{\lambda_1 l}{u_0}, \tag{2.25}$$

where λ_1 and l represent the reaction rate and characteristic length.

2.19.12 Peclet number

The non dimensionl number used in calculations involving convective heat transfer. It is the proportion of the thermal energy convected to the liquid to the thermal energy conducted within the liquid. Mathematically,

$$Pe = \frac{\lambda w_c}{D_n} \tag{2.26}$$

where λ denote the porosity parameter w_c represent constant maximum cell swimming speed and D_n represent Diffusivity of microorganism.

2.20 Conservation laws

A measurable quantity that remains unchanged with the progression of time in an isolated system is called conserved quantity and the law which deals with this quantity is recognized as conservation law. The conservation laws that are used for the flow specification in the subsequential analysis are given below.

2.20.1 Mass conservation law

Conservation law for mass states that mass of the system remain conserved. Mathematically

$$\frac{D\rho}{Dt} + \rho\boldsymbol{\nabla}.\mathbf{V} = 0, \tag{2.27}$$

or

$$\frac{\partial\rho}{\partial t} + (\mathbf{V}.\boldsymbol{\nabla})\,\rho + \rho\boldsymbol{\nabla}.\mathbf{V} = 0, \tag{2.28}$$

or

$$\frac{\partial\rho}{\partial t} + \boldsymbol{\nabla}.\,(\rho\mathbf{V}) = 0. \tag{2.29}$$

The above is equation of continuity. For the steady flow Eq. (2.29) becomes

$$\boldsymbol{\nabla}.\,(\rho\mathbf{V}) = 0, \tag{2.30}$$

and for the incompressible fluid, Eq. (2.30) will be stated as:

$$\boldsymbol{\nabla}.\mathbf{V} = 0. \tag{2.31}$$

2.21 Momentum conservation law

This law states that the total momentum remains constant of the system. Generally, it is given by:

$$\rho\frac{D\mathbf{V}}{Dt} = \operatorname{div}\boldsymbol{\tau} + \rho\mathbf{b}, \tag{2.32}$$

here $\boldsymbol{\tau} = -\mathbf{pI} + \mathbf{S}$, the Cauchy stress tensor, $\frac{D}{Dt}$ represents the material time derivative and $\mathbf{b}$ stands for body force.

2.21.1 Law of energy conservation

This states that the whole energy is conserved at the whole system. For nanofluids it is specified by :

$$\rho_f c_f \frac{DT}{Dt} = \tau^*.L^* + k\nabla^2 T + \rho_p c_p \left(D_B \nabla C.\nabla T + \frac{DT}{T_\infty} \nabla T.\nabla T \right), \tag{2.33}$$

here ρ_f represents the base liquid density, τ^* the stress tensor, ρ_p denotes the density of nanoparticles, c_f stands for specific heat of base fluid, D_B denotes the Brownian diffusivity, L^* for the strain tensor, D_T represents the thermophoretic diffusion coeffiecient, k denotes the thermal conductivity and T for temperature.

2.21.2 Law of conservation of concentration

For nanoparticles, the volume fraction equation is

$$\frac{\partial C}{\partial t} + \mathbf{V}.\boldsymbol{\nabla}\mathbf{C} = -\frac{1}{\rho_p} \boldsymbol{\nabla}.\mathbf{j}_p, \tag{2.34}$$

$$\mathbf{j}_p = -\rho_p D_B \nabla C - \rho_p D_T \frac{\nabla T}{T_\infty} \tag{2.35}$$

$$\frac{\partial C}{\partial t} + \mathbf{V}.\boldsymbol{\nabla}\mathbf{C} = \mathbf{D}_B \boldsymbol{\nabla}^2\mathbf{C} + \mathbf{D}_T \frac{\boldsymbol{\nabla}^2 T}{T_\infty}. \tag{2.36}$$

Here, D_B, C, T and D_T stand for Brownian diffusivity, nanoparticle concentration, temperature and thermophoretic coefficients respectively.

Chapter 3

A numerical analysis for nonlinear radiation in MHD flow around a cylindrical surface with chemically reactive species

In this chapter, the analysis of MHD flow for nonlinear radiation over a cylindrical surface is discussed numerically. Flow analysis is performed in the existence of chemical reaction. In addition, partial slip boundary conditions are also involved. The requisite boundary layer equations are modified into nonlinear ODEs after using suitable similarity transformation. The obtained system of linear equations is solved by bvp4c built-in function of MATLAB scheme. The outcomes of the prominent parameters versus involved profiles are portrayed and conversed in the light of their physical significance.

3.1 Mathematical analysis

We examine an incompressible flow outside a circular hollow cylinder having radius R and the constant temperature T_w. As the $x-$axis is directed via the axis of cylinder while $r-$axis is directed in the radial direction. A stretching surface of the cylinder has velocity $u_w = u_0\left(x/l\right).$

where u_0 shows the reference velocity l is the characteristics length. The flow situation induced by magnetic field of intensity B_0 shown in Fig. 3.1. Owing to our assumption of small Reynolds number, the induced magnetic field is neglected. The protuberance scale is lesser as compare to the thickness of the boundary layer so the partial slip conditions are handled. In addition, the flow field carries the chemically reactive species.

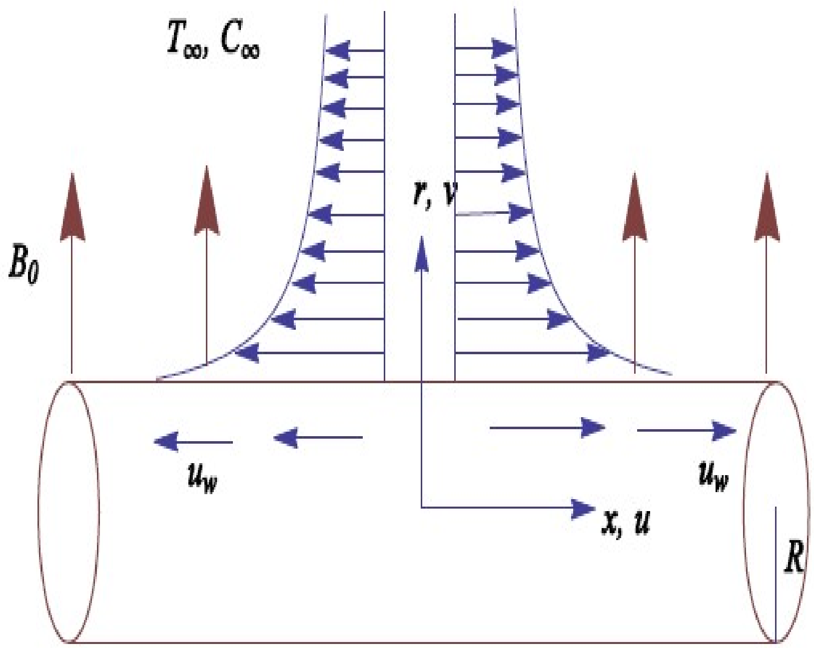

Fig. 3.1 Geometry of the flow

The resulting equations of boundary layer defining the depicted scenario are given as:

$$(ru)_x + (rv)_r = 0, \tag{3.1}$$

$$uu_x + vu_r = \upsilon \left(u_{rr} + \frac{1}{r} u_r \right) - \frac{\sigma_1}{\rho} \beta_0^2 u, \tag{3.2}$$

$$uT_x + vT_r = \frac{k}{\rho c_p} \left(T_{rr} + \frac{1}{r} T_r \right) - \nabla . q_r, \tag{3.3}$$

$$uC_x + vC_r = D_m \left(C_{rr} + \frac{1}{r} C_r \right) - \lambda_1 (C - C_\infty)^n. \tag{3.4}$$

with suitable boundary coditions

$$u\left(x,R\right)=u_w+L_1 \upsilon u_r|_{r=R},\quad v\left(x,R\right)=0,$$

$$T\left(x,R\right)=T_w+L_2T_r|_{r=R,}\ \ C\left(x,R\right)=C_w+L_3C_r|_{r=R}, \tag{3.5}$$

$$u\left(x,+\infty\right)=0,\quad T\left(x,+\infty\right)=T_\infty,\quad C\left(x,+\infty\right)=C_\infty. \tag{3.6}$$

Via Rosseland approximation, radiative heat flux q_r is denoted as:

$$q_r=\left(\frac{-4\sigma^*}{3k^*}\right)\frac{\partial T^4}{\partial r}=\left(-\frac{16\sigma^*}{3k^*}\right)T^3T_r. \tag{3.7}$$

Non dimensionl form of above mathematical model is obtained by using these transformations:

$$\eta=\frac{r^2-R^2}{2R}\left(\frac{u_0}{l\upsilon}\right)^{\frac{1}{2}},\quad \psi=\left(\frac{\upsilon u_0}{l}\right)^{\frac{1}{2}}xRf\left(\eta\right),$$

$$\theta\left(\eta\right)=\frac{T-T_\infty}{T_w-T_\infty},\quad \phi\left(\eta\right)=\frac{C-C_\infty}{C_w-C_\infty}. \tag{3.8}$$

Here, satisfaction of Eq. (3.1) is inevitable. However, Eqs. (3.2) – (3.6) take the form :

$$\left[\left(1+2M\eta\right)f^{''}\right]^{'}+ff^{''}-f^{'^2}-K^2f^{'}=0, \tag{3.9}$$

$$\frac{1}{\mathrm{Pr}}\left[\left(1+\frac{4}{3}Rd\left(1+\left(\theta_w-1\right)\theta\right)^3\right)\left(1+2M\eta\right)\theta^{'}\right]^{'}+f\theta^{'}=0, \tag{3.10}$$

$$\frac{1}{Sc}\left[\left(1+2M\eta\right)\phi^{'}\right]^{'}+f\phi^{'}-\gamma\phi^n=0, \tag{3.11}$$

$$f\left(0\right)=0,f'\left(0\right)=1+B_1f''\left(0\right),\theta\left(0\right)=1+B_2\theta'\left(0\right),\phi\left(0\right)=1+B_3\phi'\left(0\right), \tag{3.12}$$

$$f'\left(+\infty\right)=0,\theta\left(+\infty\right)=0,\phi\left(+\infty\right)=0. \tag{3.13}$$

The values of above mentioned parameters are :

$$M=\left(\frac{l\upsilon}{u_0R^2}\right)^{\frac{1}{2}},\ K=\left(\frac{\sigma_1B_0^2l}{\rho u_0}\right)^{\frac{1}{2}},B_1=L_1\left(\frac{u_0\upsilon}{l}\right)^{\frac{1}{2}},\ B_2=L_2\left(\frac{u_0}{l\upsilon}\right)^{\frac{1}{2}},$$

$$B_3 = L_3 \left(\frac{u_0}{l\upsilon}\right)^{\frac{1}{2}}, \quad Rd = \frac{4\sigma^* T_\infty^3}{kk^*}, \quad \theta_w = \frac{T_w}{T_\infty}, \quad \gamma = \frac{\lambda_1 l}{u_0}, Sc = \frac{\upsilon}{D_B}, \Pr = \frac{\upsilon}{\alpha} \tag{3.14}$$

The dimensional form of Skin friction cofficient, local Nusselt number, local Sherwood number are constructed below:

$$C_{f_x} = \frac{\mu\left(u_r + v_x\right)_{r=R}}{\rho u_w^2}, \quad Nu_x = \frac{x q_w}{k\left(T_w - T_\infty\right)},$$

$$Sh_x = \frac{x j_w}{D_m\left(C_w - C_\infty\right)}. \tag{3.15}$$

Substituting the usual similarity transformation, we get the dimensionless form of C_{f_x}, Nu_x, Sh_x

$$\mathrm{Re}_x^{\frac{1}{2}} C_{f_x} = f''(0), Nu_x \mathrm{Re}_x^{-\frac{1}{2}} = -[1 + \frac{4}{3} Rd\{1 + (\theta_w - 1)\theta(0)\}]^3 \theta'(0)$$

$$\mathrm{Re}_x^{-\frac{1}{2}} Sh_x = -\phi'(0). \tag{3.16}$$

3.2 Results and deliberation

The current portion addresses the results of different parameters on temperature, velocity components and concentration fields. Numerous parameters like the magnetic parameter K, Schmidt number Sc, temperature ratio parameter θ_w, radiation parameter Rd, Prandtl number Pr, curvature parameter M, wall roughness parameter B_1, concentration slip parameter B_3, Thermal slip parameter B_2, chemical reaction parameter γ, reaction order n are discussed on the temperature, velocity and nanoparticles concentration field. The change of velocity component on the magnetic interaction parameter K is illustrated in Fig. 3.2. This parameter K calculates the firmness of Lorentz force. The increase in K, increases the firmness of this force. Due to increase in K, the velocity in axial direction will reduce the boundary layer and hence velocity gradient is raised. The effect of wall roughness parameter B_1 on $f'(\eta)$ is shown in $Fig.$3.3. Slip decreases the velocity close to the disk and this phenomenon is more enhanced by the increase in K. Practically, the effects of stretched cylinder are transmitted to the liquid layers due to which decrease in velocity field is seen. The effect of the temperature ratio parameter θ_w on $\theta(\eta)$ is explained via Fig. 3.4. A significant increase in $\theta(\eta)$ is observed. The increase in θ_w enhances the temperature of the wall which results in thicker penetration depth for temperature profile. Also the change in temperature changes the thermal diffusivity in the boundary layer. Thermal boundary layer corresponds to be thicker close to the wall where the temperature is larger while it is lower far to the cylinder because here temperature is comparatively low. As a result, an inflection point emerge on the wall when altimately θ_w is accounted greater. The temperature profiles of the distinct parameter of curvature M are shown in Fig. 3.5. The increse in curvature parameter reduces the radius which in results increases the temperature. Fig. 3.6 is illustrated to show the plotes of $\theta(\eta)$ for distinct terms of Rd at other variables are fixed. The increase in radiation parameter enhances the thermal boundary layer which is non-identical to linear radiation flux case where temperature has a value $\mathrm{N}_r \rightarrow \infty$. In Fig. 3.7 we introduce the temperature plot with variations of Prandtl numbers. It is necessary to select the suitable Pr to obtain the expected cooling rate. In many calculations Pr=7 is used that is of water. The choosed range of the Pr is defined by the existing papers on the flows of boundary layer. In the liquid heat penetrates in less space as Pr enhances. In the liquid where Pr is greater, the thermal diffusivity is smaller than the momentum diffusivity. Therefore, an increment in the Pr is expected to raise the rate of heat transfer. Fig. 3.8 provides the change of the $\phi(\eta)$ as the Schmidt number Sc varies. Schmidt number is the ratio of momentum to mass diffusivities. With the increase of schmidt number Sc the mass diffusivities decreases and results in the depletion of concentration profile $\phi(\eta)$. We therefore expect that an enhancement in Sc would decrease the concentration thickness. Fig. 3.9 shows the change of the reaction rate parameter γ on the field of ϕ. As expected, the increase rate of chemical reaction results in a decline of $\phi(\eta)$. Fig. 3.10 shows the change in the concentration profile $\phi(\eta)$ as the reaction rate n varies. The layer of concentration increases when the greater order chemical reaction is considered.

We considered non linear radiative flow of heat transfer by MHD caused by a cylinder by applying the partial slip conditions on the wall. Temperature, velocity and concentration fields over the cylinder are calculated in the system for the complete limitations of the slip parameters. The validation of the current calculation scheme was performed by relating the outcomes of wall shear stress with the available parameters and such resemblance proved to be effective (see table 3.1). In tables 3.2 and 3.3 the calculation of the heat transfer rate $\mathrm{Re}_x^{-1/2} Nu_x$ and the local Sherwood number $\mathrm{Re}_x^{-1/2} Sh_x$ are presented with numerous parameter variations. Its noticeable that local Nusselt number enhances with the enhancing variations of curvature parameter M. The heat transfer rate is reduced as the effect of magnetic field increases. Also concluded that the heat transfer coefficient could also be enhanced by the reduction of the cylinder's radius. At rising variations of θ_w or Rd, an elevation with the rate of heat transfer is shown. The maximum improvement of the local Sherwood number is expressed as the Schmidt value is enlarged. Practically, when the Schmidt values increases, momentum diffusion become demonstrative by the mass diffusion and as a outcome the thickness of the concentration's boundary layer lowers. These findings in a greater mass transfer rate. In addition,the enlarging reaction rate has a capacity to decrease the rate of mass transfer.

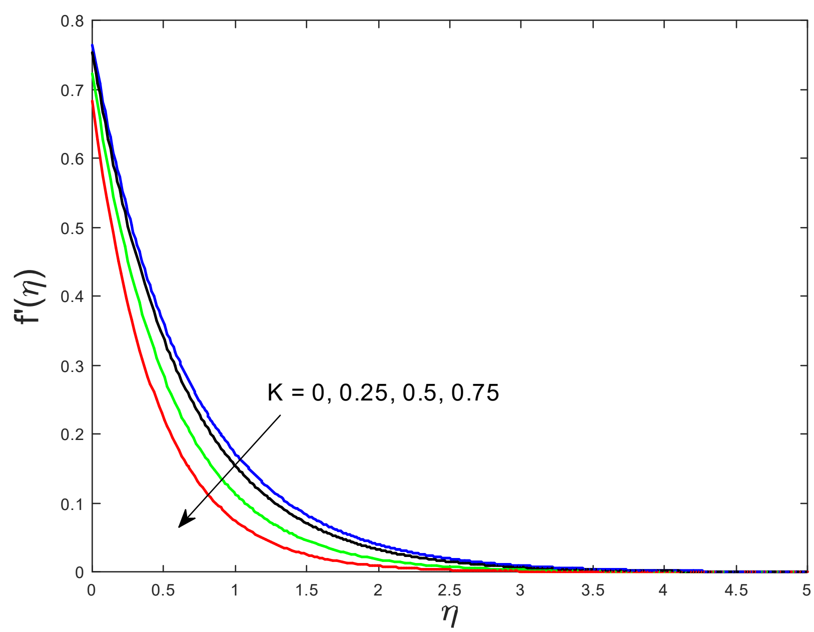

$Fig.3.2$: Impact of magnetic parameter K on $f'(\eta)$

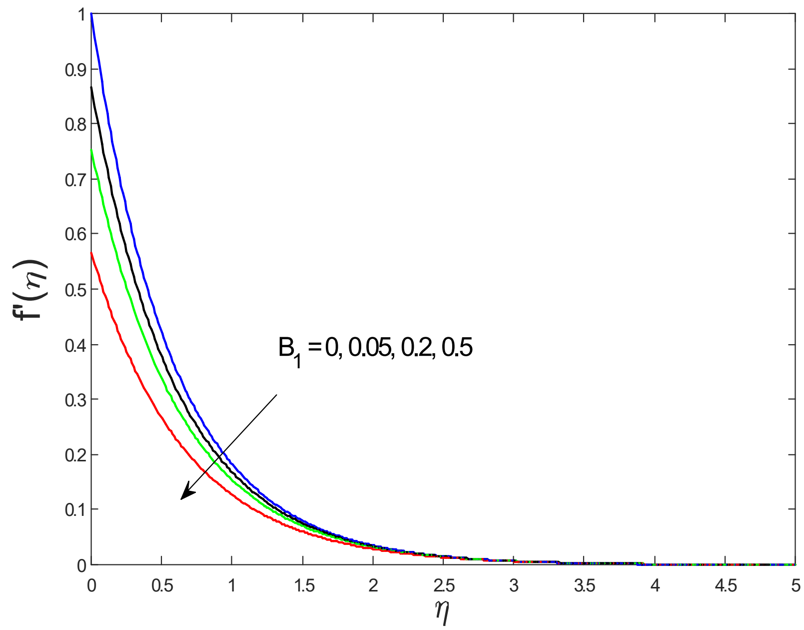

$Fig.3.3$: Impact of wall roughness parameter B_1 on $f'(\eta)$

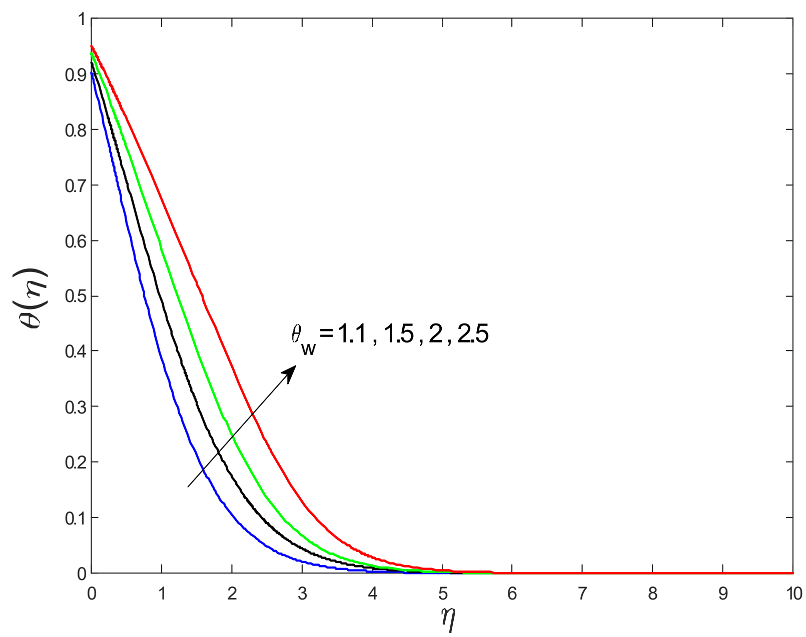

$Fig.3.4$: Impact of temperature ratio parameter θ_w on $\theta(\eta)$

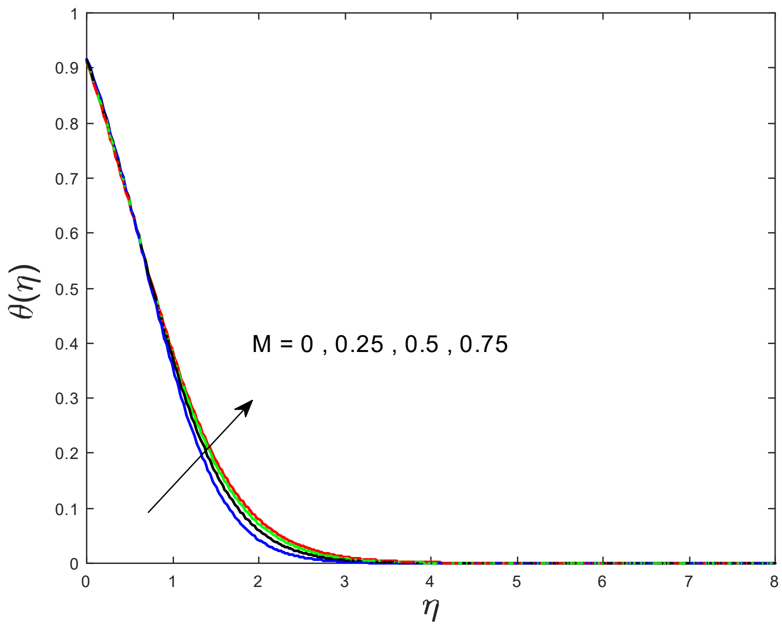

$Fig.3.5$: Impact of curvature parameter M on $\theta\left(\eta\right)$

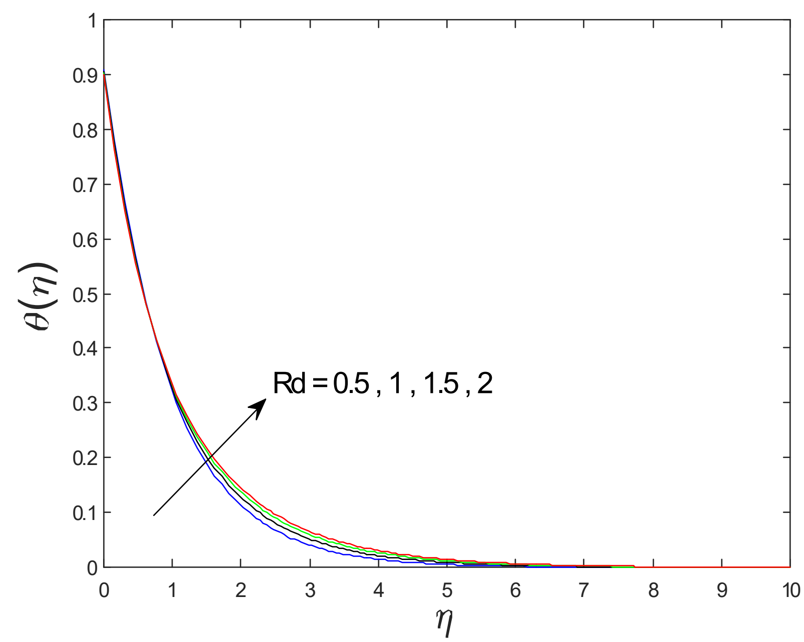

$Fig.3.6$: Impact of radiation parameter Rd on $\theta\left(\eta\right)$

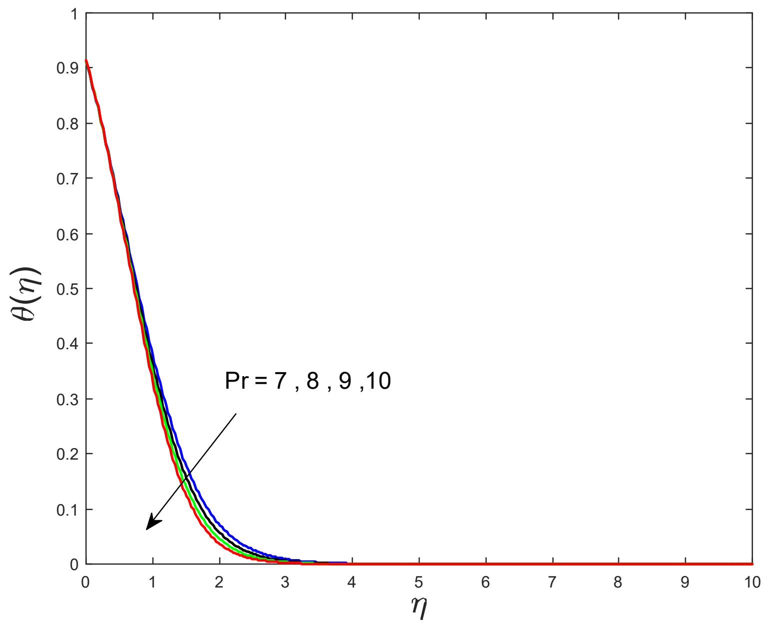

$Fig.3.7$: Impact of prandtl number Pr on $\theta\,(\eta)$

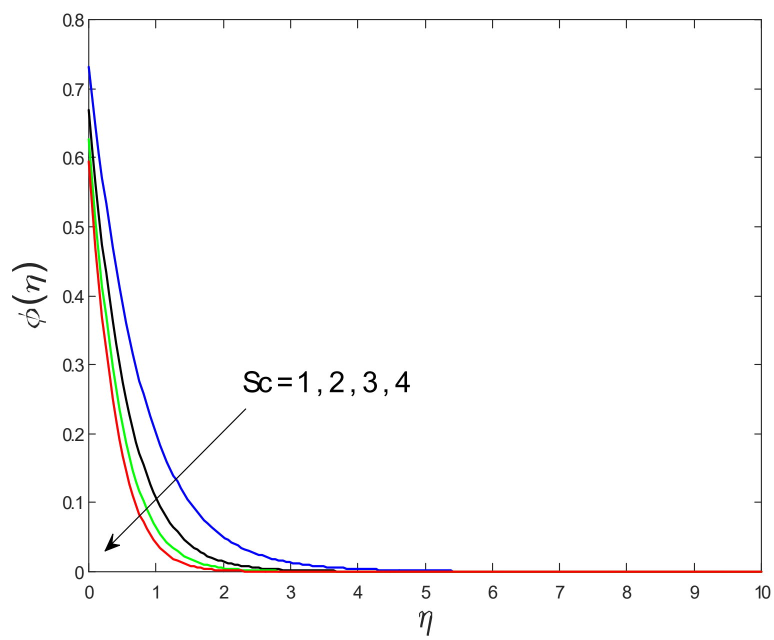

$Fig.3.8$: Impact of schmidt number Sc on $\phi\,(\eta)$

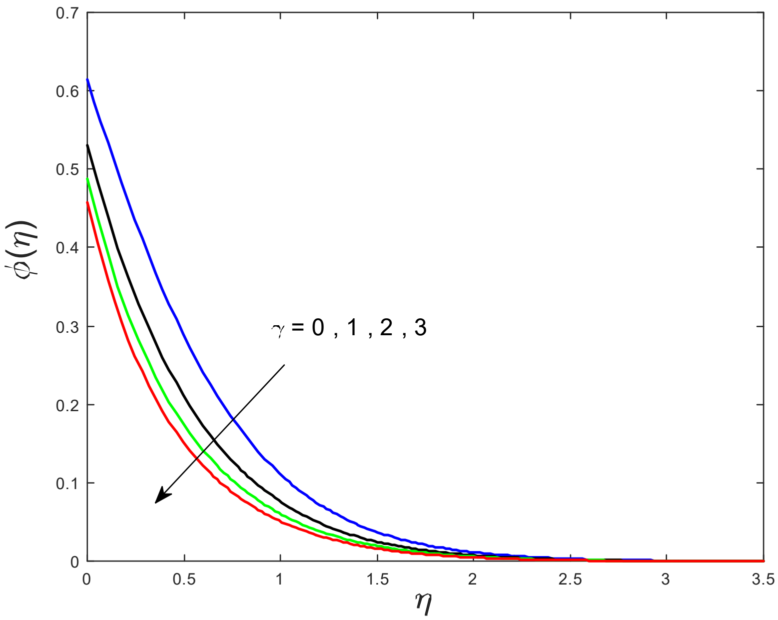

$Fig.3.9$: Impact of chemical reaction parameter γ on $\phi(\eta)$

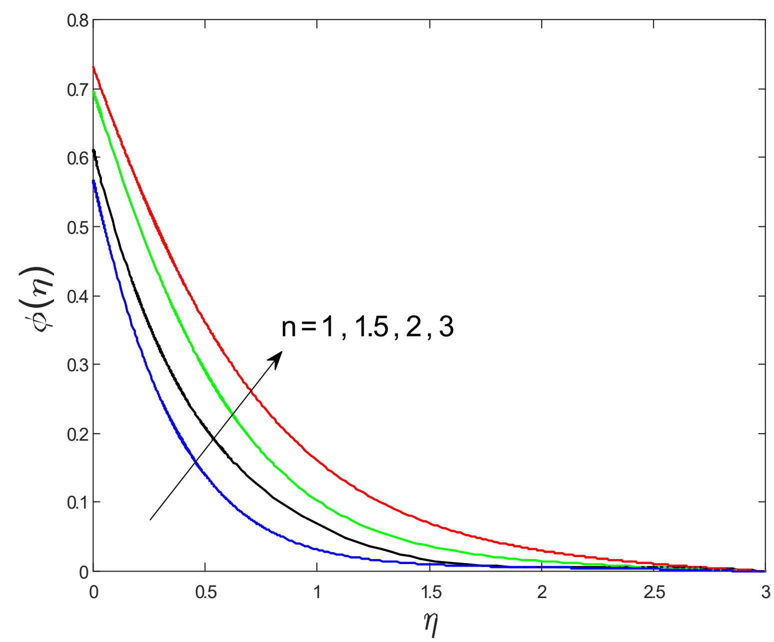

$Fig.3.10$: Impact of Reaction order parameter n on $\phi(\eta)$

Table 3.1 : Validation of numerical results for $-f''(0)$ with those of Tamoor et. al. [43] when $M = B_1 = 0$.

	$-f''(0)$	$-f''(0)$	$-f''(0)$
K	Tamoor et.al.[43]	Junaid Ahmad khan	Present
0	1	1	1
0.2	1.01980	1.0198039	1.01981
0.5	1.11803	1.1180340	1.11803
0.8	1.28063	1.2806248	1.28062
1	1.41421	1.4142136	1.41421

Table 3.2 :Computations of $(\mathrm{Re}_x)^{-\frac{1}{2}} Nu_x$ for various variations of K, M, θ_w and Rd when $\mathrm{Pr} = 7$ and $B_1 = B_2 = 0.5$.

K	M	$\theta_w = A$	Rd	$(\mathrm{Re}_x)^{-\frac{1}{2}} Nu_x$
0.5	0.2	1.5	0.2	0.7654
1				0.6803
1.5				0.5851
2				0.5003
	0.5			0.7745
	0.7			0.7801
	1			0.7883
		2		1.1440
		2.5		1.4871
		3		1.7770
			0.1	1.3736
			0.3	2.2339
			0.5	3.3713

Table 3.3 : Computations of $(\mathrm{Re}_x)^{-\frac{1}{2}} Sh_x$ for various variations of M, Sc and γ when $Pr = 7$, $k = 0.5$ an $B_1 = B_2 = B_3 = 0.5$.

M	Sc	γ	n	$(\mathrm{Re}_x)^{-\frac{1}{2}} Sh_x$
0.2	5	1	1	1.15817
0.5				1.1748
0.7				1.18683
1				1.20568
	2			0.975654
	3			1.05478
	7			1.22726
		2		1.27036
		3		1.34142
		4		1.39264
			2	0.996419
			3	0.924968
			5	0.878547

Chapter 4

Nonlinear Radiative MHD Williamson nanofluid flow over a stretching cylinder in a Darcy-Forchheimer porous medium

In this chapter, a nonlinear radiative MHD Williamson nano-liquid stream via a stretched cylinder in a Darcy-Forchheimer porous media is discussed. Besides, The envisioned model is supported by the slip, Convective and zero-mass flux boundary conditions at the surface of the cylinder. The requisite boundary layer equations are converted into the nonlinear ODEs after the use of suitable transformation. The obtained system of linear equations is solved by bvp4c built-in function of MATLAB scheme. The outcomes of the prominent parameters versus involved profiles are portrayed and conversed in light of their physical significance.

4.1 Mathematical analysis

We examin an incompressible flow outside a circular hollow cylinder having radius R and the constant temperature T_w. As the $x-$axis is axial direction of cylinder while $r-$axis is directed in the direction of radial. A stretching surface of the cylinder has velocity $u_w = u_0\left(x/l\right)$, where

u_0 shows the reference velocity l is the characteristics length. The flow situation induced by magnetic field of intensity B_0 shown in Fig. 4.1.

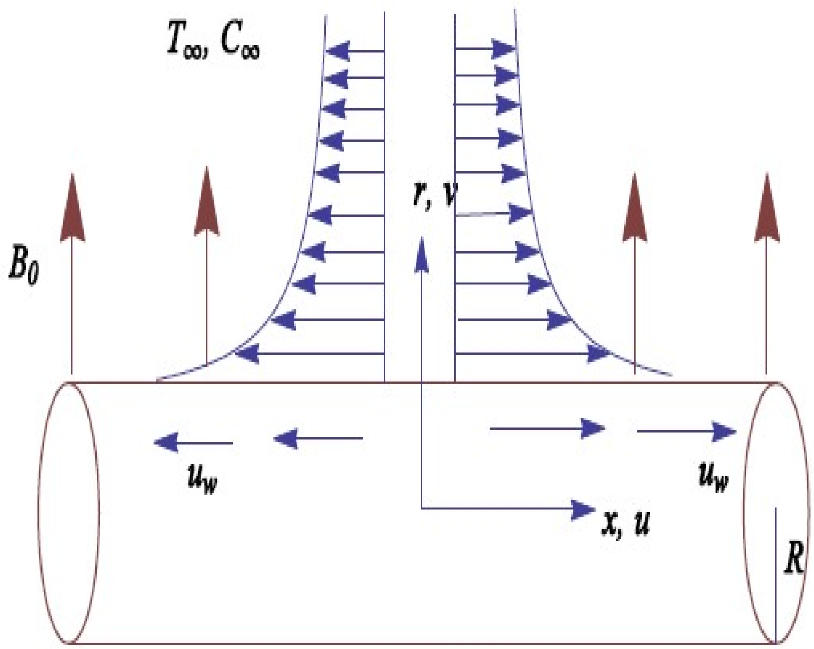

Fig. 4.1 Geometry of the flow

The resulting boundary layer equations defining the depicted scenario are given as:

$$(ru)_x + (rv)_r = 0, \tag{4.1}$$

$$uu_x + vu_r = \upsilon\left(u_{rr} + \frac{1}{r}u_r + 2\Gamma u_r u_{rr} + \frac{\Gamma}{\sqrt{2}r}(u_r)^2\right) - \frac{\sigma_1}{\rho}\beta_0^2 u - \frac{\upsilon}{k_2}u - Fu^2, \tag{4.2}$$

$$uT_x + vT_r = \frac{k}{\rho c_p}\left(T_{rr} + \frac{1}{r}T_r\right) + \tau\left[D_B T_r C_r + \frac{D_T}{T_\infty}(T_r)^2\right] - \frac{1}{\rho c_p}(q_r)_r, \tag{4.3}$$

$$uC_x + vC_r = D_B\left(C_{rr} + \frac{1}{r}C_r\right) + \frac{D_T}{T_\infty}\left(T_{rr} + \frac{1}{r}T_r\right) - \lambda_1(C - C_\infty)^n, \tag{4.4}$$

$$uN_x + vN_r = D_n\left(N_{rr} + \frac{1}{r}N_r\right) - \frac{\lambda w_c}{C_w - C_\infty}\left[N_r C_r + NC_{rr}\right]. \tag{4.5}$$

with suitable boundary coditions

$$u(x, R) = u_w\ ,\ v(x, R) = 0,$$

$$T(x,R)=T_w,\ C(x,R)=C_w,$$

$$u(x,+\infty)=0\ ,\ T(x,+\infty)=T_\infty\ ,\ C(x,+\infty)=C_\infty,$$

$$N(x,R)=N_w,\quad N(x,+\infty)=N_\infty. \tag{4.6}$$

Via Rosseland approximation, the radiative heat flux is q_r is given as:

$$q_r=\left(\frac{-4\sigma^*}{3k^*}\right)\frac{\partial T^4}{\partial r}=\left(\frac{-16\sigma^*}{3k^*}\right)T^3T_r. \tag{4.7}$$

Non dimensionl form of the above mathematical model is obtained by using these transformations:

$$\eta=\frac{r^2-R^2}{2R}\left(\frac{u_0}{l\upsilon}\right)^{\frac{1}{2}},\quad \psi=\left(\frac{\upsilon u_0}{l}\right)^{\frac{1}{2}}xRf(\eta)\quad ,\theta(\eta)=\frac{T-T_\infty}{T_w-T_\infty},$$
$$\phi(\eta)=\frac{C-C_\infty}{C_w-C_\infty},\quad \zeta(\eta)\ =\frac{N-N_\infty}{N_w-N_\infty},\quad u=\frac{u_0}{l}xf'(\eta),\ v=-\frac{1}{r}\sqrt{\frac{\upsilon u_0}{l}}Rf(\eta). \tag{4.8}$$

Here, satisfaction of Eq. (4.1) is inevitable. However, Eqs. (4.2) – (4.6) take the form

$$(1+2M\eta)f'''+ff''-f'^2+2Mf''+2We(1+2M\eta)^{\frac{3}{2}}f''f'''+3WeM(1+2M\eta)^{\frac{1}{2}}f''^2$$
$$-K^2f'-\lambda f'-Frf'^2=0, \tag{4.9}$$

$$\frac{1}{\Pr}\left[(1+2M\eta)\theta''+2M\theta'\right]+f\theta'+Nb(1+2M\eta)\theta'\phi'+Nt(1+2M\eta)\theta'^2$$
$$+\frac{1}{\Pr}\frac{4}{3}Rd\left[\begin{array}{c}3\left[1+(\theta_w-1)\theta\right]^2(\theta_w-1)(1+2M\eta)\theta'^2+\left[1+(\theta_w-1)\theta\right]^3M\theta'\\+\left[1+(\theta_w-1)\theta\right]^3(1+2M\eta)\theta''\end{array}\right]=0, \tag{4.10}$$

$$(1+2M\eta)\phi''+2M\phi'+Scf\phi'+\frac{Nt}{Nb}\left[(1+2M\eta)\theta''+2M\theta'\right]-Sc\gamma\phi^n=0, \tag{4.11}$$

$$(1+2M\eta)\zeta''+2M\zeta'+Lb\Pr f\zeta'$$
$$\left[-Pe\begin{array}{c}(1+2M\eta)\zeta'\phi'+\sigma M\phi'+(1+2M\eta)\zeta\phi''\\M\zeta\phi'+\sigma(1+2M\eta)\phi''\end{array}\right]=0. \tag{4.12}$$

$$f(0)=0, f'(0)=1, \theta(0)=1,$$

$$\phi(0)=1, \zeta(0)=1,$$

$$f'(+\infty)=0, \theta(+\infty)=0, \phi(+\infty)=0, \zeta(+\infty)=0. \tag{4.13}$$

The variations of the above mentioned parameters are :

$$M=\left(\frac{\upsilon l}{u_0 R^2}\right)^{\frac{1}{2}}, K=\left(\frac{\sigma_1 B_0^2 l}{\rho u_0}\right)^{\frac{1}{2}}, \theta_w=\frac{T_w}{T_\infty}, \gamma=\frac{\lambda_1 l}{u_0},$$

$$Nb=\frac{\tau D_B(C_w-C_\infty)}{\upsilon},\ Nt=\frac{\tau D_T(Tw-T_\infty)}{\upsilon T_\infty}, We=\frac{\Gamma u_0^{\frac{3}{2}} x}{\sqrt{2\upsilon} l^{\frac{3}{2}}},$$

$$\lambda=\frac{\upsilon l}{k_2 u_0}, Fr=\frac{c_b}{\sqrt{k_2}},\ Rd=\frac{4\sigma^* T_\infty^3}{kk^*}, Sc=\frac{\upsilon}{D_B},$$

$$Pe=\frac{\lambda w_c}{D_n},\ P_r=\frac{\upsilon}{\alpha}, L_b=\frac{\alpha}{D_n}, \sigma=\frac{N_\infty}{N_w-N_\infty}. \tag{4.14}$$

The dimensional form of Skin friction, local Nusselt number, local Sherwood number and Motile microorganisms are given by:

$$C_{f_x}=\frac{\tau_w}{\rho u_w^2}, Nu_x=\frac{xq_w}{k(T_w-T_\infty)}, Sh_x=\frac{xj_w}{D_m(C_w-C_\infty)}, Nn_x=\frac{xq_n}{D_n \Delta N}, \tag{4.15}$$

where

$$\tau_w=\mu\left(\frac{\partial u}{\partial r}+\frac{\Gamma}{\sqrt{2}}\left(\frac{\partial u}{\partial r}\right)^2\right)_{r=R},\ q_w=-k\left(\frac{\partial T}{\partial r}\right)_{r=R}+(q_r)_w, \tag{4.16}$$

$$j_w=-D_m\left(\frac{\partial C}{\partial r}\right)_{r=R}, \qquad q_n=-D_n\left(\frac{\partial N}{\partial r}\right)_{r=a}.$$

Substituting the usual similarity transformation we get the Dimensionless form of $C_{f_x}, Nu_x, Sh_x, Nn_x$

$$\mathrm{Re}_x^{\frac{1}{2}} C_{f_x}=f''(0)+Wef''^2(0),\ Nu_x \mathrm{Re}_x^{-\frac{1}{2}}=-\left[1+\frac{4}{3}Rd\{1+(\theta_w-1)\theta(0)\}\right]^3\theta'(0)$$

$$\mathrm{Re}_x^{-\frac{1}{2}} Sh_x=-\phi'(0),\ Nn_x=-\xi'(0). \tag{4.17}$$

4.2 Results and deliberation

This portion is devoted to depict the effect of different physical parameters on velocity, concentration and temperature fields. The various parameters of the magnetic interaction parameter K, Darcy parameter Fr, the temperature ratio parameter θ_w, radiation parameter Rd, Schmidt number Sc, porosity parameter λ, Local Weissenberg number We, thermophoresis parameter Nt, curvature parameter M, bioconvection Lewis number Lb, Prandtl number Pr, Brownian motion parameter Nb, chemical reaction parameter γ, Peclet number Pe, Bioconvection parameter σ and reaction order n are discussed on temeparature, velocity, and nanoparticles concentration profiles. Fig. 4.2. depicts the behavior of magnetic interaction parameter K on the velocity profile. The magnetic interaction parameter K measures a strength of Lorentz force. The increase in K enhances the Lorentz force strength and due to rise in K the velocity in axial direction decreases the boundary layer. As a result, the gradient of velocity at the surface is decreased. The Impact of Darcy parameter Fr on velocity field $f'(\eta)$ is investigated in Fig. 4.3. It is examined that by escalating the variations of Fr, the decreasing behavior of the velocity field is seen. This is because the higher values of Fr produces resistance in a fluid flow and hence velocity decreases. Fig. 4.4 portrays the trend of the porosity number λ on the velocity distribution of $f'(\eta)$. The liquid's velocity diminishes on greater values of porosity parameter. Physically, the movement of the fluid is hindered due to the presence of porous media and this results in the fall off the fluid velocity. The impact of Weissenberg number We on velocity field $f'(\eta)$ is investigated in Fig. 4.5. It is examined that by escalating the variations of We, the decreasing behaviour of the velocity field is seen. The explaination behind it is that the fluid relaxation time increases by increasing the value of We number, which creates resistance to the fluid and therefore fluid velocity decreases. The effect of the ratio parameter θ_w upon $\theta(\eta)$ is explained by Fig. 4.6. A significant increase in $\theta(\eta)$ is observed. Enhancing θ_w signifies the temperature of the wall that causes thicker penetration depth for temperature profile. Also the thermal diffusivity lies in the boundary layer with the relating temperature change. Thermal boundary layer corresponds to be thicker nearby the wall where the temperature is larger while it is lower far from cylinder because here temperature is low as compared to others. As a result, an inflection point emerge on the wall when greater θ_w is considered. The temperature field for numerous curvature parameters M are shown in Fig. 4.7. A substantial enhancement in liquid temperature is seen when radius of cylinder is reduced. The influence of Prandtl number Pr on the temperature field is described in Fig. 4.8. It is observed that the existence of melting phenomenon of the liquid temperature increases with rising variations of Prandtl number Pr. Therefore, we can judge that greatter variations of the Prandtl number Pr enhances the temperature profile. Figure 4.9 is drawn to show the plotes of $\theta(\eta)$ for numerous terms of Rd when other variables are fixed. It can be a judged that growing values of Rd enhances the temperature and its parallel thickness of layer become thicker. Substantially, it is clear that in the radiation procedure, heat is created in the working liquid, which causes an enhancement in the thermal profile. Figure 4.10 elucidates that an increment in Schmidt number Sc decays the nanoparticle concentration distribution $\phi(\eta)$. There is an opposite relationship of the Schmidt number and the Brownian diffusion coefficient. Greater the values of Schmidt number Sc lower will be the Brownian diffusion coefficient, which tends to decrease the $\phi(\eta)$. Fig. 4.11 portrays the concentration field for different estimations of chemical reaction parameter γ. Large variations of the chemical reaction parameter γ tends to reduce the nanoparticle concentration field. Fig. 4.12 shows that for greater values of reaction order n the concentration profile becomes higher. Fig. 4.13 depicts the impact of thermophoresis parameter Nt on concentration profile $\phi(\eta)$. Both the concentration and thermal layer thickness are increased by increasing the variations of the thermophoresis parameter Nt. Greater estimations of the thermophoresis parameter Nt give rise to thermophoresis force which increases the movement of nanoparticles from cold to hot surfaces and also increases in the thermal layer thickness. The decending behavior in concentration distribution $\phi(\eta)$ against Brownian motion parameter Nb is drawn in fig. 4.14. An enhancement in the Brownian motion parameter Nb increases the Brownian motion due to which there is an increase in the movement of nanoparticles and hence boundary layer thickness reduces. Fig. 4.15 plotted to draw the curves of $\zeta(\eta)$ for different terms of bioconvection Lewis number Lb while other variables are fixed. It is observed that Lb depicts the decreasing behavior for large values of Lb. Fig. 4.16 shows the behavior of Peclet number Pe on gyrotactic microorganisms profile $\zeta(\eta)$. Here, $\zeta(\eta)$ is an increasing function of Pe that effects to a decrease the diffusivity of microorganisms. Fig. 4.17 indicates the variations in gyrotactic microorganism profile $\zeta(\eta)$ for distinct estimations of the bio-convection parameter σ. Large variations of bio-convection parameter decreases the gyrotactic microorganism field. In addition, Tables $(4.1 - 4.3)$ shows that the numerical variations of the local Sherwood number Sh_x, local Nusselt number Nu_x and density amount of motile microorganism Nn_x for distinct estimations of K, M, θ_w, Rd, Pr, Sc, γ, k, Pe, Lb, and σ.

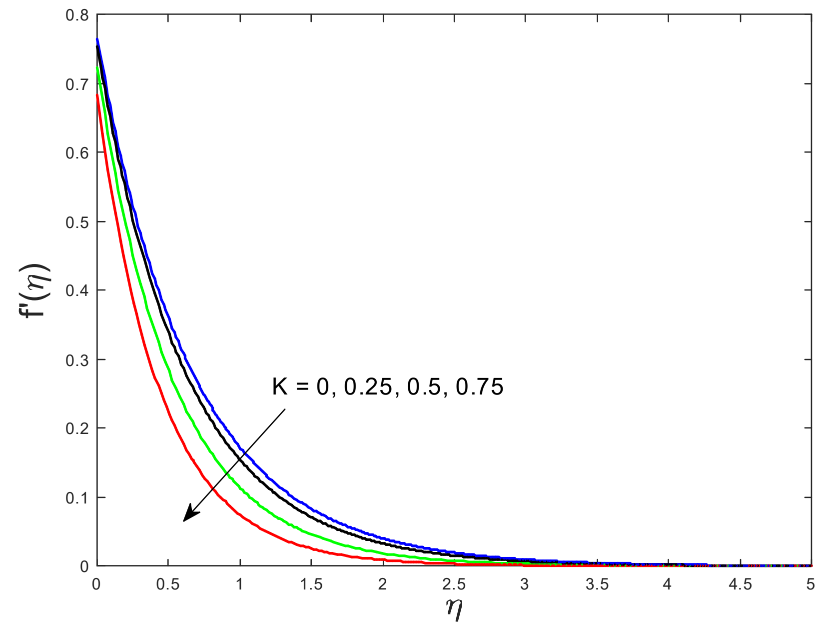

$Fig.4.2$: Impact of magnetic parameter K on $f'(\eta)$

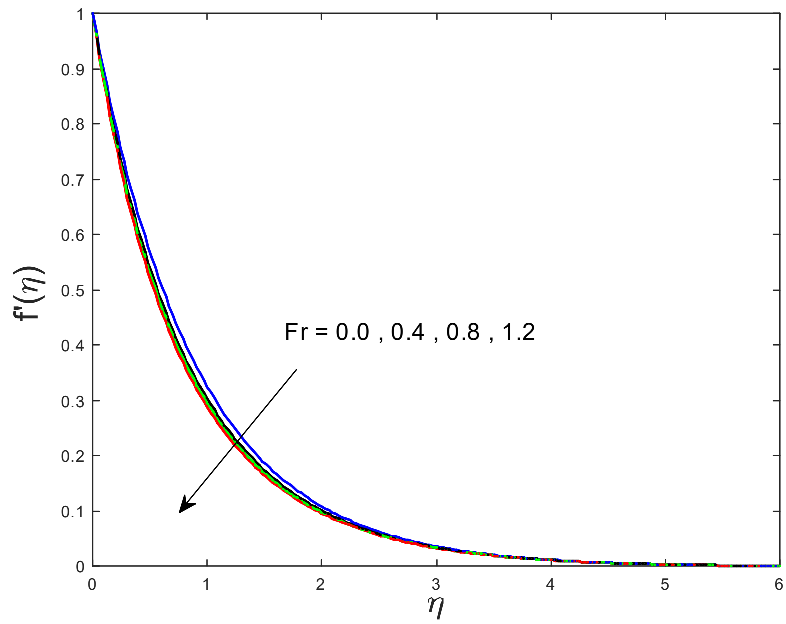

$Fig.4.3$: Impact of Darcy parameter Fr on $f'(\eta)$

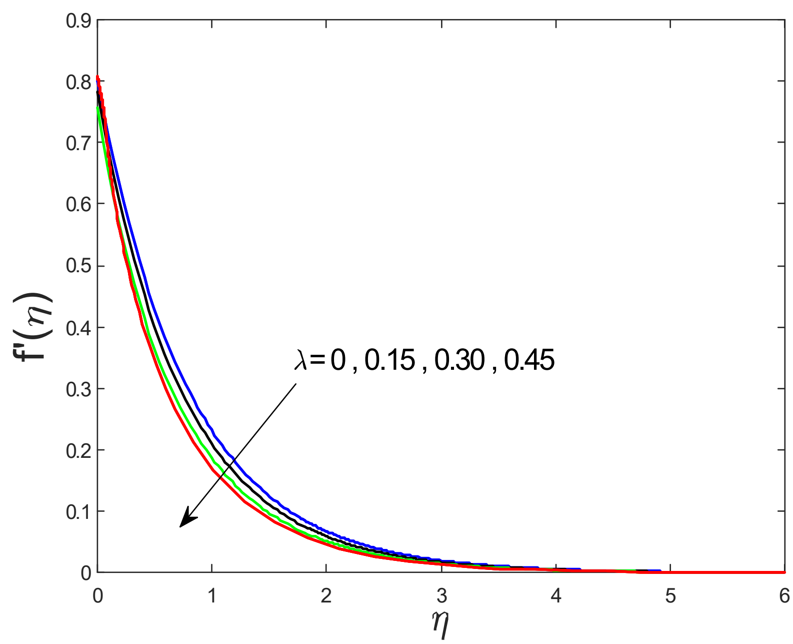

$Fig.4.4$: Impact of porosity parameter λ on $f'(\eta)$

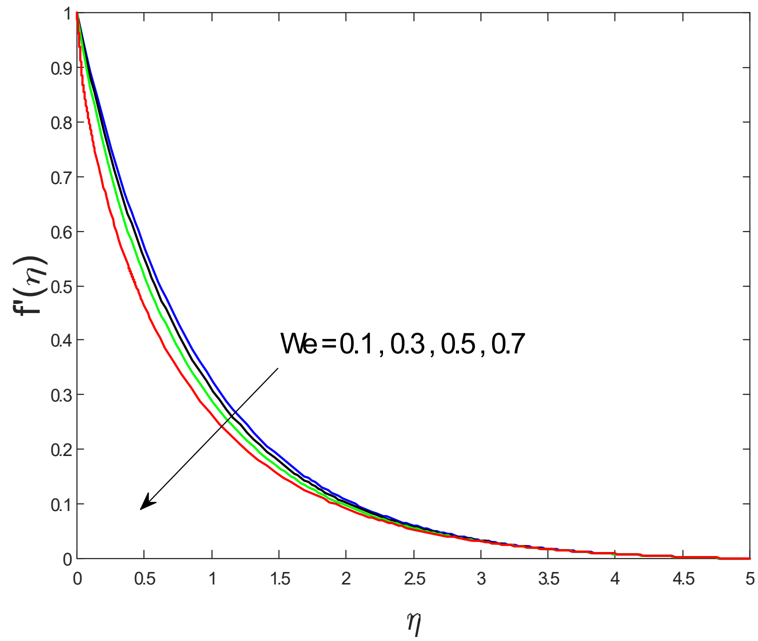

$Fig.4.5$: Impact of Local Weissenberg number We on $f'(\eta)$

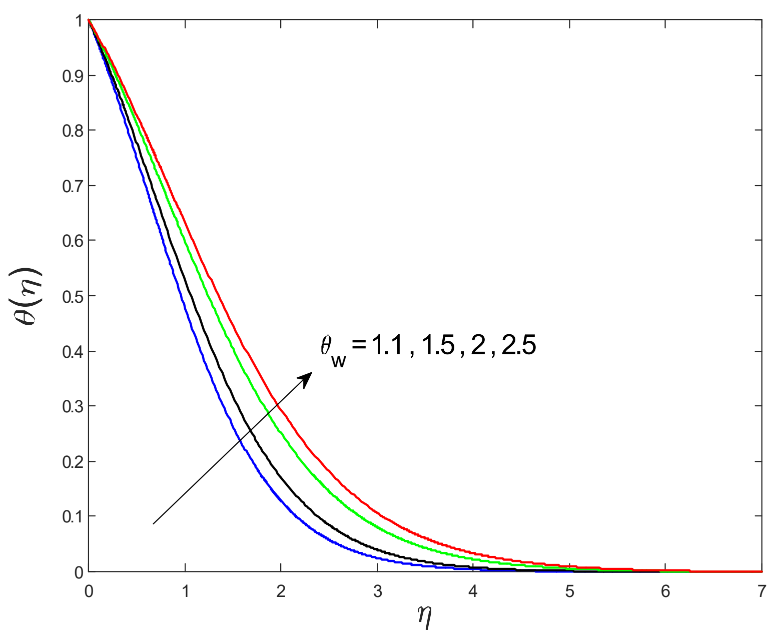

$Fig.4.6$: Impact of temperature ratio parameter θ_w on $\theta(\eta)$

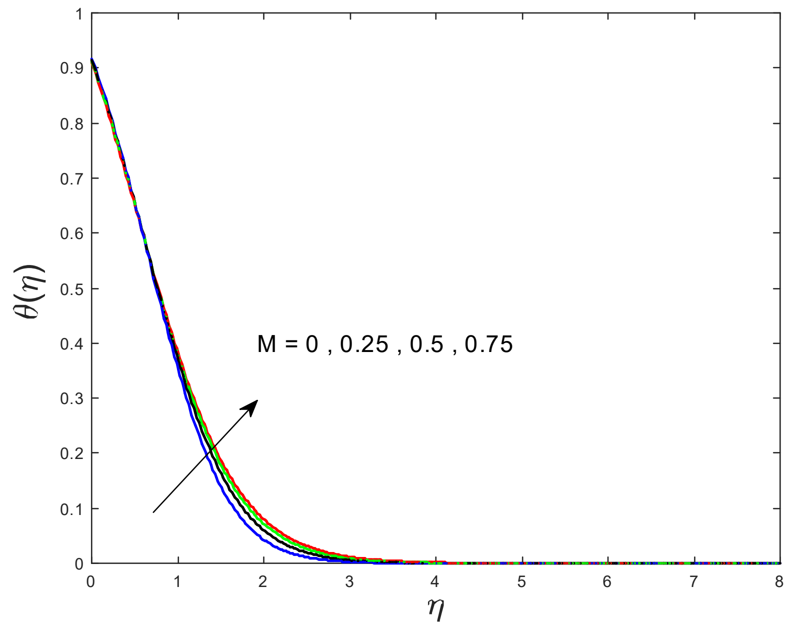

$Fig.4.7$: Impact of curvature parameter M on $\theta(\eta)$

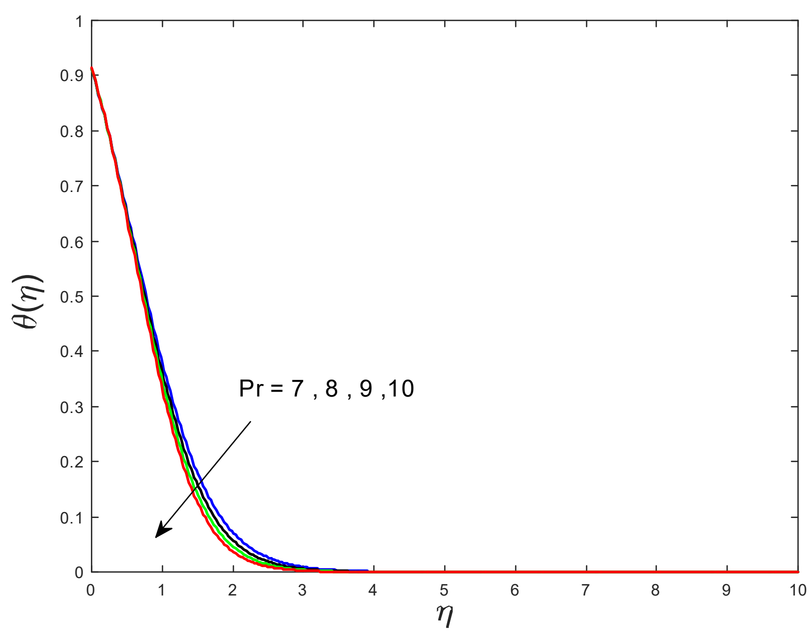

$Fig.4.8$: Impact of prandtl number Pr on $\theta(\eta)$

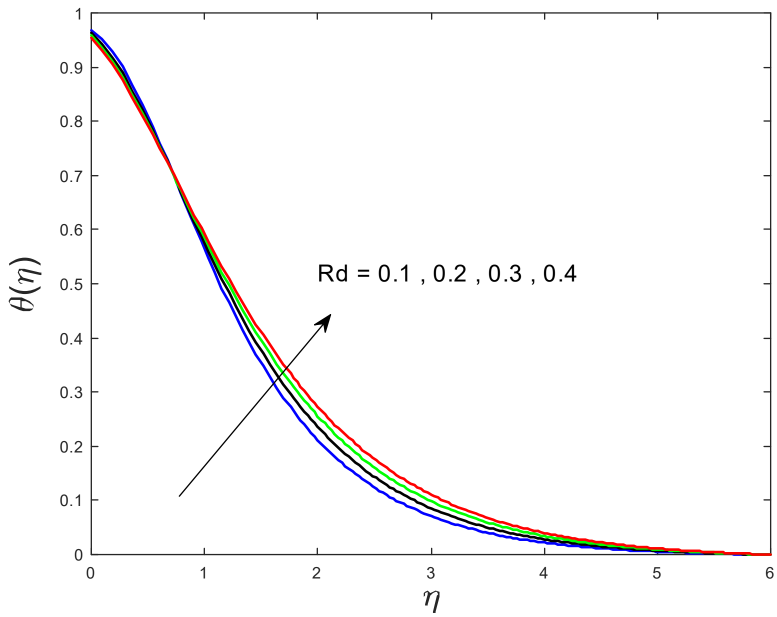

$Fig.4.9$: Impact of radiation parameter Rd on $\theta\,(\eta)$

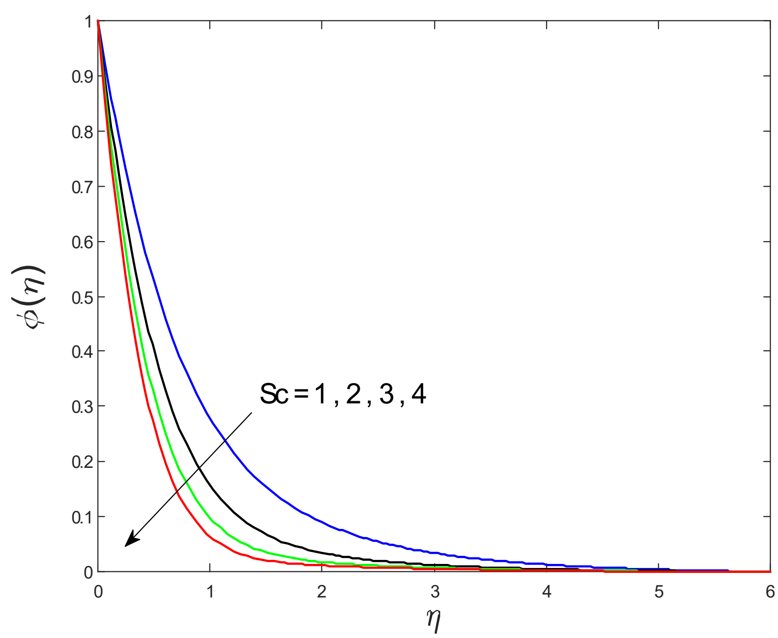

$Fig.4.10$: Impact of Schmidt number Sc on $\phi\,(\eta)$

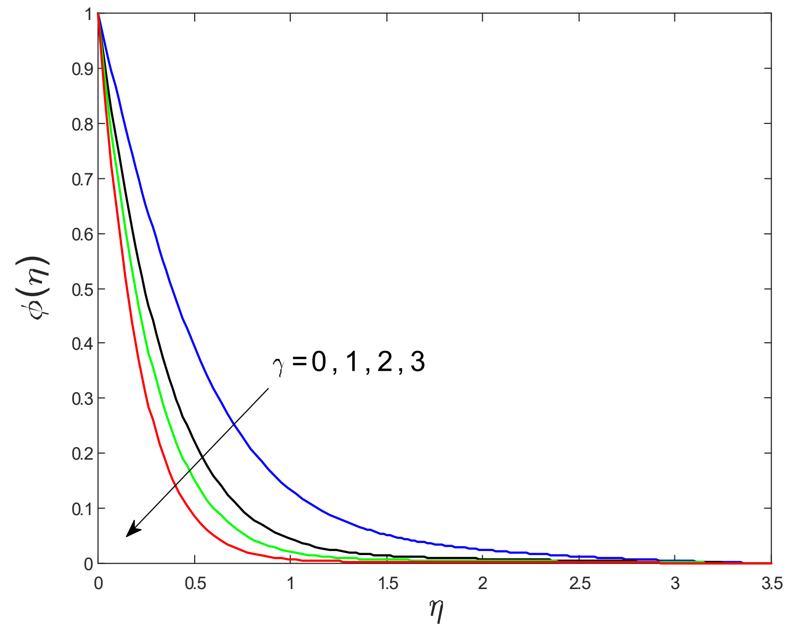

$Fig.4.11$: Impact of Chemical reaction parameter γ on $\phi\,(\eta)$

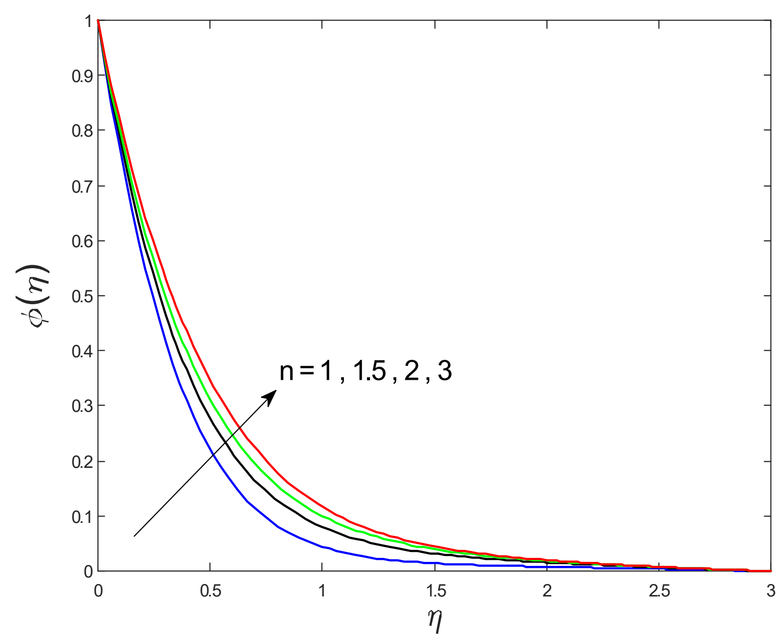

$Fig.4.12$: Impact of reaction order n on $\phi\,(\eta)$

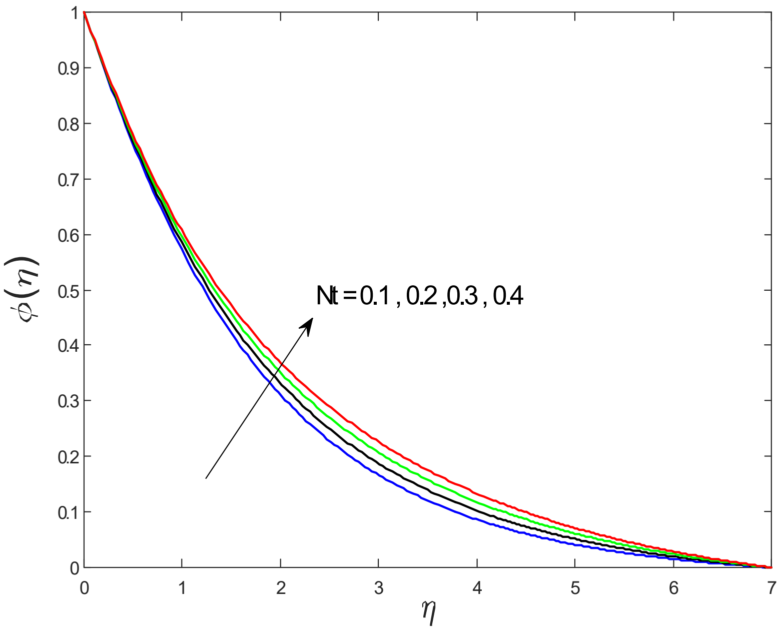

$Fig.4.13$: Impact of thermophoresis parameter Nt on $\phi\left(\eta\right)$

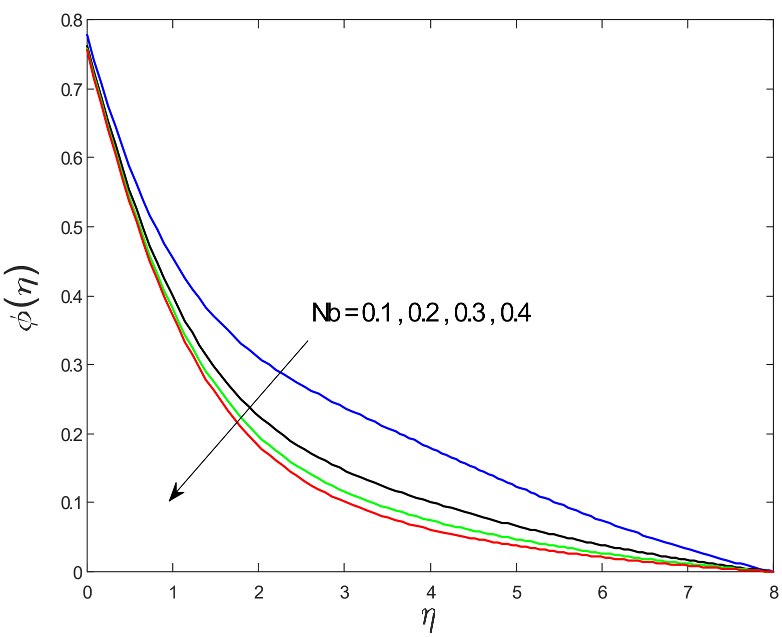

$Fig.4.14$: Impact of Brownian motion parameter Nb on $\phi\left(\eta\right)$

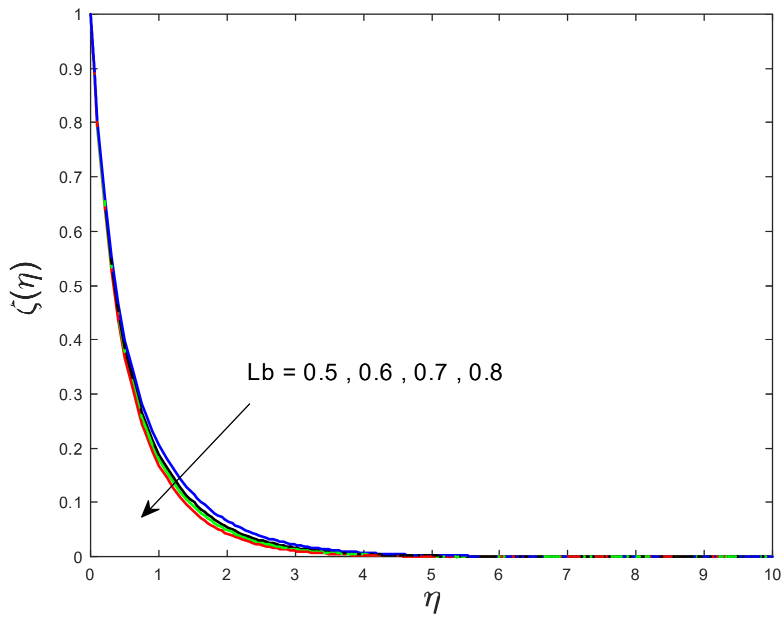

$Fig.4.15$: Impact of Bioconvection lewis number Lb on $\xi\,(\eta)$

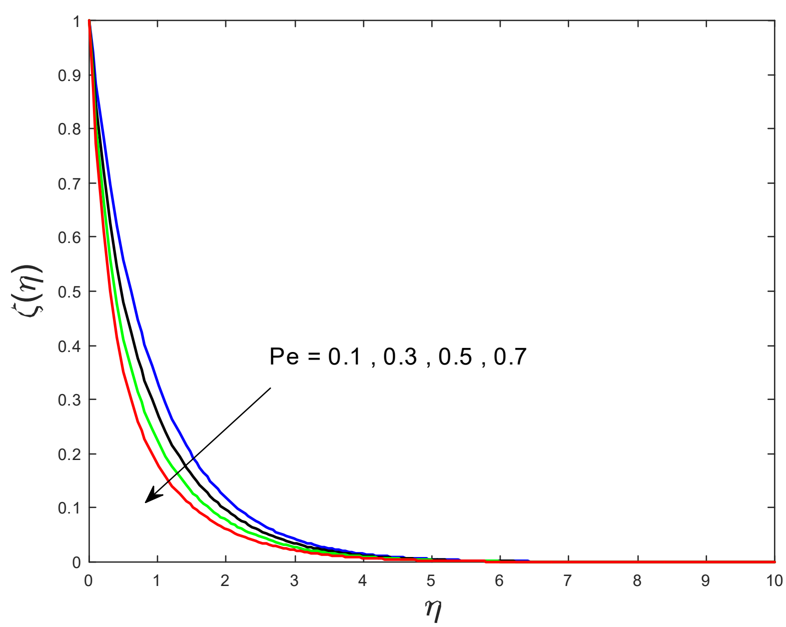

$Fig.4.16$: Impact of peclet number pe on $\xi\,(\eta)$

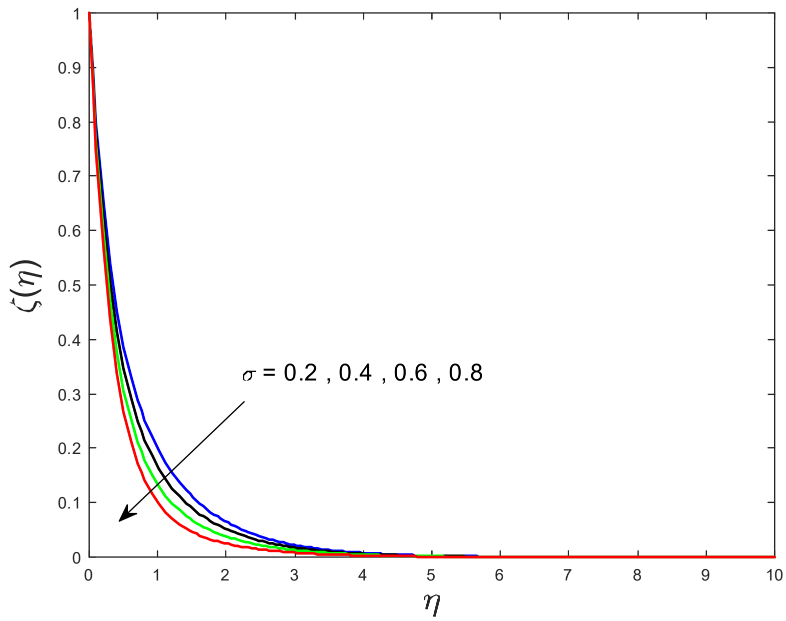

$Fig.4.17$: Impact of Bioconvection parameter σ on $\xi(\eta)$

Table 4.1 :Computations of $(\mathrm{Re}_x)^{-1/2} Nu_x$ for various variations of K, M, θ_w and Rd when $\mathrm{Pr} = 7$.

K	M	$\theta_w = A$	Rd	$(\mathrm{Re}_x)^{-\frac{1}{2}} Nu_x$
0.5	0.2	1.5		0.7654
1				0.6803
1.5				0.5851
2				0.5003
	0.5			0.7745
	0.7			0.7801
	1			0.7883
		2		1.1440
		2.5		1.4871
		3		1.7770
			0.1	1.3736
			0.3	2.2339
			0.5	3.3713

Table 4.2 : Computations of $(\mathrm{Re}_x)^{-\frac{1}{2}}Sh_x$ for various variations of M, Sc and γ when $Pr = 7$, $k = 0.5$.

M	Sc	γ	n	$(\mathrm{Re}_x)^{-\frac{1}{2}}Sh_x$
0.2	5	1	1	1.15817
0.5				1.1748
0.7				1.18683
1				1.20568
	2			0.975654
	3			1.05478
	7			1.22726
		2		1.27036
		3		1.34142
		4		1.39264
			2	0.996419
			3	0.924968
			5	0.878547

Table 4.3 : Computations of $(\mathrm{Re}_x)^{-\frac{1}{2}} Nn_x$ for various variations of M, Pr, σ, Pe, and Lb.

M	Pr	σ	Pe	Lb	$(\mathrm{Re}_x)^{-\frac{1}{2}} Nn_x$
0.3	1.5	0.2	0.3	0.2	
0.3					0.935596
0.6					1.05958
0.9					1.1936
	1.0				0.915801
	1.5				0.935596
	2.0				0.940771
		0.2			0.935596
		0.4			1.01258
		0.6			1.08956
			0.4		1.06529
			0.5		1.18901
			0.6		1.30713
				0.3	0.963155
				0.6	1.03821
				0.9	1.10378

Chapter 5

Concluding remarks and Future work

In this thesis model, two problems have been analyzed where first problem is about review paper and second problem is the extension work for it. Conclusions of both the problems are as following:

5.1 Chapter 3

A numerical investigation for non-linear radiation in the flow of MHD around a surface of cylindrical with chemically reactive species. The main outcomes of this analysis are listed below:

- Velocity distribution is lower for large variations of the magnetic interaction parameter K.
- Large values of temperature ratio parameter θ_w, radiation parameter Rd, and curvature parameter M, causes an increment in temperature distribution.
- Enhancing variations of Prandtl number Pr shows the decending behavior on temperature field.
- An increment in Schmidt number Sc and chemical reaction parameter γ leads to lower

concentration profile.

- Concentration field enhanses for greater variations of reaction order n.

5.2 Chapter 4

In the current investigation, we have discussed non linear radiative MHD Williamson nano liquid flow via a stretched cylinder in a Darcy-Forchheimer porous media. Solution of the problem is addressed by Matlab scheme of bvp4c built-in function. The main features of the current investigation are appended below:

- Velocity distribution is lower for large variations of .magnetic interaction parameter K, Darcy parameter Fr, and porosity parameter λ.
- Larger values of temperature ratio parameter θ_w, radiation parameter Rd, and curvature parameter M, causes an increment in temperature distribution.
- Enhancing variations of Prandtl number Pr shows the decreasing behavior on temperature profile.
- An increment in Schmidt number Sc and chemical reaction parameter γ leads to lower concentration profile.
- Brownian motion parameter Nb and thermophoresis parameter Nt shows the different behavior on concentration field.
- Peclet number Pe decrease the gyrotactic microorganism profile.
- Gyrotactic microorganism profile reduces for greater variations of bioconvection Lewis number Lb and bioconvection parameter σ.

5.3 Future work

The recent analysis could be extended to the following models as well:

- The fluid flow may be extended to the any other non-Newtonian fluid.
- The Buongiorno nanofluid model may be swapped with Tiwari and Das model.
- Some varied types of base fluids and nano-materials may be used.
- Some different non-Newtonian fluid model may also be considered.
- Effect of Hall current and Dusty fluid may also be considered.

Bibliography

[1] Choi, S. U. S., & Eastman, J. A. (1995). Enhancing thermal conductivity of fluids with nanoparticles. ASME Int Mech Eng Congr Expo 66: 99–105.

[2] Koo, J., & Kleinstreuer, C. (2005). Laminar nanofluid flow in microheat-sinks. International Journal of Heat and Mass Transfer, 48(13), 2652-2661.

[3] Eastman, J. A., Choi, S. U. S., Li, S., Yu, W., & Thompson, L. J. (2001). Anomalously increased effective thermal conductivities of ethylene glycol-based nanofluids containing copper nanoparticles. Applied Physics Letters, 78(6), 718-720.

[4] Choi, S. U. S., Zhang, Z. G., Yu, W., Lockwood, F. E., & Grulke, E. A. (2001). Anomalous thermal conductivity enhancement in nanotube suspensions. Applied Physics Letters, 79(14), 2252-2254.

[5] Ramzan, M., Bilal, M., & Chung, J. D. (2017). Radiative Williamson nanofluid flow over a convectively heated Riga plate with chemical reaction-A numerical approach. Chinese journal of Physics, 55(4), 1663-1673.

[6] Hayat, T., Aziz, A., Muhammad, T., & Alsaedi, A. (2017). Darcy–Forchheimer three-dimensional flow of Williamson nanofluid over a convectively heated nonlinear stretching surface. Communications in Theoretical Physics, 68(3), 387.

[7] Sheikholeslami, M., Arabkoohsar, A., & Jafaryar, M. (2020). Impact of a helical-twisting device on the thermal–hydraulic performance of a nanofluid flow through a tube. Journal of Thermal Analysis and Calorimetry, 139(5), 3317-3329.

[8] Yang, L., Huang, J. N., Ji, W., & Mao, M. (2020). Investigations of a new combined application of nanofluids in heat recovery and air purification. Powder Technology, 360, 956-966.

[9] Li, F., Sheikholeslami, M., Dara, R. N., Jafaryar, M., Shafee, A., Nguyen-Thoi, T., & Li, Z. (2020). Numerical study for nanofluid behavior inside a storage finned enclosure involving melting process. Journal of Molecular Liquids, 297, 111939.

[10] Li, F., Sheikholeslami, M., Dara, R. N., Jafaryar, M., Shafee, A., Nguyen-Thoi, T., & Li, Z. (2020). Numerical study for nanofluid behavior inside a storage finned enclosure involving melting process. Journal of Molecular Liquids, 297, 111939.

[11] Komeilibirjandi, A., Raffiee, A. H., Maleki, A., Nazari, M. A., & Shadloo, M. S. (2020). Thermal conductivity prediction of nanofluids containing CuO nanoparticles by using correlation and artificial neural network. Journal of Thermal Analysis and Calorimetry, 139(4), 2679-2689.

[12] Gupta, S., Kumar, D., & Singh, J. (2020). Analytical study for MHD flow of Williamson nanofluid with the effects of variable thickness, nonlinear thermal radiation and improved Fourier's and Fick's Laws. SN Applied Sciences, 2(3), 1-12.

[13] Kebede, T., Haile, E., Awgichew, G., & Walelign, T. (2020). Heat and Mass Transfer in Unsteady Boundary Layer Flow of Williamson Nanofluids. Journal of Applied Mathematics, 2020.

[14] Rasool, G., Zhang, T., Chamkha, A. J., Shafiq, A., Tlili, I., & Shahzadi, G. (2020). Entropy Generation and Consequences of Binary Chemical Reaction on MHD Darcy–Forchheimer Williamson Nanofluid Flow Over Non-Linearly Stretching Surface. Entropy, 22(1), 18.

[15] Khan, S. U., Shehzad, S. A., & Ali, N. (2020). Bioconvection flow of magnetized Williamson nanoliquid with motile organisms and variable thermal conductivity. Applied Nanoscience, 1-12.

[16] Darcy, H. (1856). Les fontaines publiques de la ville de Dijon: exposition et application... Victor Dalmont.

[17] Forchheimer, P. (1901). Wasserbewegung durch boden. Z. Ver. Deutsch, Ing., 45, 1782-1788.

[18] Muskat, M. (1946). The ‡ow of homogeneous ‡uids through porous media (No. 532.5 M88).

[19] Pal, D., & Mondal, H. (2012). Hydromagnetic convective diffusion of species in Darcy–Forchheimer porous medium with non-uniform heat source/sink and variable viscosity.International Communications in Heat and Mass Transfer, 39(7), 913-917.

[20] Ganesh, N. V., Hakeem, A. A., & Ganga, B. (2016). Darcy–Forchheimer flow of hydromagnetic nanofluid over a stretching/shrinking sheet in a thermally strati…ed porous medium with second order slip, viscous and Ohmic dissipations effects. Ain Shams Engineering Journal, 9(4) 939-951.

[21] Alshomrani, A. S., & Ullah, M. Z. (2019). E¤ects of Homogeneous–Heterogeneous Reactions and Convective Condition in Darcy–Forchheimer Flow of Carbon Nanotubes. Journal of Heat Transfer, 141(1), 012405.

[22] Saif, R. S., Hayat, T., Ellahi, R., Muhammad, T., & Alsaedi, A. (2018). Darcy–Forchheimer flow of nanofluid due to a curved stretching surface. International Journal of Numerical Methods for Heat & Fluid Flow. DOI: 10.1108/HFF-08-2017-0301.

[23] Seth, G. S., Kumar, R., & Bhattacharyya, A. (2018). Entropy generation of dissipative flow of carbon nanotubes in rotating frame with Darcy-Forchheimer porous medium: A numerical study. Journal of Molecular Liquids, 268, 637-646.

[24] Hayat, T., Ra…que, K., Muhammad, T., Alsaedi, A., & Ayub, M. (2018). Carbon nanotubes significance in Darcy-Forchheimer flow. Results in physics, 8, 26-33.

[25] Zeeshan, A., Maskeen, M. M., & Mehmood, O. U. (2018). Hydromagnetic nanofuid flow past a stretching cylinder embedded in non-Darcian Forchheimer porous media. Neural Computing and Applications, 30(11), 3479-3489.

[26] Tarakaramu, N., Narayana, P. S., & Venkateswarlu, B. (2019). MHD Three Dimensional Darcy-Forchheimer Flow of a Nanofluid with Nonlinear Thermal Radiation. In Applied Mathematics and Scientific Computing, 87-97.

[27] RamReddy, C., Naveen, P., & Srinivasacharya, D. (2018). nonlinear convective flow of non-Newtonian fuid over an inclined plate with convective surface condition: a Darcy–Forchheimer model. International Journal of Applied and Computational Mathematics, 4(1), 51.

[28] Farooq, M., Ahmad, S., Javed, M., & Anjum, A. (2019). Melting heat transfer in squeezed nanofluid flow through Darcy Forchheimer medium. Journal of Heat Transfer, 141(1), 012402.

[29] Zeeshan, A., Shehzad, N., & Ellahi, R. (2018). Analysis of activation energy in Couette-Poiseuille flow of nanofluid in the presence of chemical reaction and convective boundary conditions. Results in Physics, 8, 502-512.

[30] Animasaun, I. L. (2015). Dynamics of unsteady MHD convective flow with thermophoresis of particles and variable thermo-physical properties past a vertical surface moving through binary mixture. Open Journal of Fluid Dynamics, 5(02), 106.

[31] Animasaun, I. L. (2015). Effects of thermophoresis, variable viscosity and thermal conductivity on free convective heat and mass transfer of non-Darcian MHD dissipative Casson fluid flow with suction and nth order of chemical reaction. Journal of the Nigerian Mathematical Society, 34(1), 11-31.

[32] Animasaun IL. 47nm aluminawaternanofluid flow within boundary layer formed on upper horizontal surface of paraboloid of revolution in the presence of quarticautocatalysischemical reaction. Alexandria Engineering Journal 2016.

[33] Nagendramma, V., Leelarathnam, A., Raju, C. S. K., Shehzad, S. A., & Hussain, T. (2018). Doubly stratified MHD tangent hyperbolic nanofluid flow due to permeable stretched cylinder. Results in Physics, 9, 23-32.

[34] Waqas, M., Hayat, T., Shehzad, S. A., & Alsaedi, A. (2018). Transport of magnetohydrodynamic nanomaterial in a stratified medium considering gyrotactic microorganisms. Physica B: Condensed Matter, 529, 33-40.

[35] Abbasi, F. M., Shehzad, S. A., Hayat, T., & Alhuthali, M. S. (2016). Mixed convection flow of jeffrey nanofluid with thermal radiation and double stratification. Journal of Hydrodynamics, Serial B, 28(5), 840-849.

[36] Paul, A., & Deka, R. K. (2017). Unsteady natural convection flow past an infinite cylinder with thermal and mass stratification. International Journal of Engineering Mathematics, 2017.

[37] Rehman, K. U., Khan, A. A., Malik, M. Y., & Pradhan, R. K. (2017). Combined effects of Joule heating and chemical reaction on non-Newtonian fluid in double stratified medium: A numerical study. Results in Physics, 7, 3487-3496.

[38] Mishra, S. R., Pattnaik, P. K., & Dash, G. C. (2015). Effect of heat source and double stratification on MHD free convection in a micropolar fluid. Alexandria Engineering Journal, 54(3), 681-689.

[39] Krishnamurthy, M. R., Gireesha, B. J., Prasannakumara, B. C., & Gorla, R. S. R. (2016). Thermal radiation and chemical reaction effects on boundary layer slip flow and melting heat transfer of nanofluid induced by a nonlinear stretching sheet. Nonlinear Engineering, 5(3), 147-159.

[40] Sohail, M., Naz, R., & Abdelsalam, S. I. (2020). On the onset of entropy generation for a nanofluid with thermal radiation and gyrotactic microorganisms through 3D flows. Physica Scripta, 95(4), 045206.

[41] Khan, M. I., Qayyum, S., Hayat, T., Khan, M. I., & Alsaedi, A. (2019). Entropy optimization in flow of Williamson nanofluid in the presence of chemical reaction and Joule heating. International Journal of Heat and Mass Transfer, 133, 959-967.

[42] Sarojamma, G., Vijaya Lakshmi, R., Satya Narayana, P. V., & Animasaun, I. L. (2020). Exploration of the significance of autocatalytic chemical reaction and Cattaneo-Christov heat flux on the dynamics of a micropolar fluid. Journal of Applied and Computational Mechanics, 6(1), 77-89.

usman thesis

ORIGINALITY REPORT

16%	9%	14%	2%
SIMILARITY INDEX	INTERNET SOURCES	PUBLICATIONS	STUDENT PAPERS

PRIMARY SOURCES

1	Junaid Ahmad Khan, M. Mustafa. "A numerical analysis for non-linear radiation in MHD flow around a cylindrical surface with chemically reactive species", Results in Physics, 2018 Publication	2%
2	www.tandfonline.com Internet Source	2%
3	Makinde, O.D., and I.L. Animasaun. "Bioconvection in MHD nanofluid flow with nonlinear thermal radiation and quartic autocatalysis chemical reaction past an upper surface of a paraboloid of revolution", International Journal of Thermal Sciences, 2016. Publication	2%
4	worldwidescience.org Internet Source	1%
5	link.springer.com Internet Source	1%
6	www.mdpi.com Internet Source	<1%

08/09/2020